Studies in Blood-Brain Barrier Disruption in Anthrax Meningitis

A dissertation submitted in partial fulfillment of the requirements for the degree of Doctor of Philosophy at George Mason University

By

Dhritiman V. Mukherjee
Master of Science
George Mason University, 2007
Bachelor of Art
The University of North Carolina at Chapel Hill, 2000

Director: Dr. Serguei G. Popov, Professor
National Center for Biodefense and Infectious Diseases

Spring Semester 2009
George Mason University
Fairfax, VA

Copyright 2009 Dhritiman V. Mukherjee
All Rights Reserved

DEDICATION

I dedicate this dissertation to three special individuals, whose inspiration and guidance have sustained me in the pursuit of this path of knowledge: my father Dr. Sakti P. Mukherjee, mother Dr. Chhabirani Mukherjee, and GMU faculty Dr. Myung-Chul Chung. Thank you for your support.

ACKNOWLEDGEMENTS

I would like to thank my committee chair Dr. Serguei Popov, and committee members Dr. Charles Bailey, Dr. Dan N. Cox, Dr. Robert Smith and Dr. Myung-Chul Chung who have given me the opportunity, the facilities and funding to work on this research project towards my Ph.D. degree. I like to thank my fellow graduate students for all the giggles, warm friendship and support, especially Dr. Shelley Jorgensen my lab colleague and friend. I also have the pleasure to acknowledge Dr. K.S. Kim of Johns Hopkins University for providing me with the human brain microvascular endothelial cells for my investigation. A special thanks to Dr. Li Dong (George Mason University) and Donna Pierce (Johns Hopkins University) for providing technical support and Dr. Nalini Ramarao for providing the *B. subtilis* mutants. I would like to recognize U.S. Department of Defense (Grant # DAMD 17-03-C-01220) and U.S. Department of Energy (Grant # DE-FC52-FC04NA25455) for the grants that made this work possible.

TABLE OF CONTENTS

LIST OF FIGURES

LIST OF ABBREVIATIONS AND SYMBOLS

Term	Abbreviation/Symbol
Adherens-junction	AJ
Human retinal pigment epithelial cells	ARPE-19
Blood-brain barrier	BBB
Blood-retinal barrier	BRB
Central nervous system	CNS
Cerebral spinal fluid	CSF
4',6-diamidino-2-phenylindole	DAPI
Diethylaminoethyl cellulose	DEAE
Differential interference contrast	DIC
Dithiothreitol	DTT
Evans blue	EB
Electric Cell-substrate impedance sensing	ECIS
1-ethyl-3-(3-dimethylaminopropyl) carbodiimide hydrochloride	EDC
Ethylenediaminetetraacetic acid	EDTA
Edema toxin	EdTx
Fluorescein isothiocyanate	FITC
Gastrointestinal	GI
Growth regulated oncogene-alpha (CXCL-1, chemokine)	Gro
Human brain microvascular endothelial cells	HBMEC
Hank's balanced salt solution	HBSS
4-(2-hydroxyethyl)-1-piperazineethanesulfonic acid	HEPES
Histidine	HIS
Inter-cellular adhesion molecule 1	ICAM-1
Interlukin	IL
Immune-inhibitor A	InhA
Isopropyl β-D-1-thiogalactopyranoside	IPTG
Junctional adhesion molecule	JAM
Luria-Bertani	LB
Lethal toxin	LeTx
Microbial collagenase metalloprotease	M9
Membrane-associated guanylate kinase	MAGUK
Monocyte chemotactic protein-1	MCP
Monodansylcadaverine	MDC

Matrix metalloprotease……MMP
Anthrax neutral metalloproteases……. Npr599
Plasminogen activator factor……..PAF
Plasminogen activator inhibitor……..PAI
Phosphate buffer sailine……..PBS
Polymerase chain reaction……..PCR
Bacillus anthracis plasmid X01 (harbors genes for toxin production)……pX01
Bacillus anthracis plasmid X02 (harbors genes for bacterial capsule)……pX02
Radio-immunoprecipitation assay buffer……..RIPA
Recombinant zonula occludens……rZO-1
Sodium dodecyl sulfate polyacrylamide gel electrophoresis……..SDS-PAGE
Trans-endothelial/epithelial electrical resistance……TEER
Tight-junction……..……TJ
Tumor necrosis factor-alpha…… TNF-α
Tissue plasminogen activator…….……tPA
Units……U
Weight to volume……...W/V
Experimental media……XM
Zonula occludens-1…….....…ZO-1
Zonula occludens toxin…..……ZOT

ABSTRACT

STUDIES ON BLOOD-BRAIN BARRIER DISRUPTION IN ANTHRAX MENINGITIS

Dhritiman V. Mukherjee, Ph.D.

George Mason University, 2009

Dissertation Director: Dr. Serguei G. Popov

B. anthracis causes hemorrhagic meningitis. The pathogenesis and molecular mechanisms associated with blood-brain barrier (BBB) dysfunction in anthrax meningitis remain poorly understood. We reported previously that anthrax-secreted metalloprotease Immune-Inhibitor A (InhA) degrades various substrates, including extracellular matrix proteins, endogenous inhibitors, and coagulation proteins. To understand the possible role and mechanism(s) of this potential virulence factor in disruption of BBB, we investigated its effects on the integrity and permeability of human brain microvasculature endothelial cells (HBMEC), as a model of blood-endothelial barriers. A time-dependent decrease of trans-epithelial and endothelial resistance by InhA suggests that HBMEC are highly sensitive to InhA. One of the major tight junction (TJ) proteins in vascular endothelial cells, ZO-1, was found to be a molecular target of InhA treatment. ZO-1 existing in cell lysates, intact cells, and recombinant forms was effectively degraded by InhA. Inhibition

of phagocytosis by cytochalasin D and monodansylcadaverine disrupted the ZO-1 degradation, and immunostaining of InhA showed its colocalization with ZO-1 in cell periphery, strongly suggesting that InhA is delivered to target ZO-1 by phagocytosis. In addition, InhA-transformed *B. subtilis* efficiently invaded, compared to its wild type, and anti-InhA antibodies inhibited this invasion of *B. anthracis* spores into HBMEC, suggesting thereby InhA-mediated spore entry. Finally, mice challenged with purified InhA underwent the BBB leakage in a time-dependent manner. Injection of Quantum dot-conjugated InhA into mice provided further evidence that InhA is required at the BBB leakage of anthrax meningitis. These findings present a previously unknown role and mechanism of the bacterial (*B. anthracis*) protease, InhA, in CNS vascular endothelial disruption, involving a mechanism facilitated by degradation of ZO-1 by InhA. Persuasive evidence is presented of the selective targeting of the major scaffolding protein, zonulin, in brain endothelial tight junction by the anthrax-secreted metalloprotease, InhA, and its close association with increased BBB permeability and *in vivo* extravasation (hemorrhage) in brain. These observations suggest that *B. anthracis* meningitis may primarily result from disintegration of the structural organization of the junctional complex of endothelial cells by bacterial product (InhA). However, it remains uncertain whether or not direct passage of the bacterial has a role in barrier disruption. Nonetheless, the mechanism proposed adds a new dimension to our understanding of anthrax meningitis.

1. INTRODUCTION

Background and significance

Anthrax is a zoonotic disease caused by the spore-forming bacterium *Bacillus anthracis*, its potential for destructive toxicity and lethal outcome in both infected animals and the incidental human victims is a matter of grave concern for medical scientists, practitioners, and society in general. Usually infecting wild or domestic animals and incidentally infecting humans coming in contact with infected animals or animal products, the disease can be either limited to cutaneous infection, which is medically curable, or inhalational, causing serious, often fatal pulmonary infection. Veterinary epidemics amongst livestock may incur substantive economic loss; but human infections leading to fatality, even if isolated sporadic cases, may become a medical challenge.

The devastating consequences of systemic anthrax infection have come to light, unfortunately, through accidental exposure of spores in industrial or bio-weapon research establishments. Inhalation anthrax is known to cause extensive systemic hemorrhage and vasculitis, as revealed from autopsy studies. While bacterial meningitis remains one of the 10 leading causes of infection-related deaths throughout the world, only a limited number of pathogenic bacteria can actually cause this condition (1). Anthrax infections,

in its systemic dissemination, can progress into hemorrhagic meningoencephalitis, which in most cases ends fatally. Besides the serious CNS morbidity and high mortality, even the few survivors may carry extreme disabilities. From the medical standpoint, it remains highly intriguing how only a few pathogens e.g., *B. anthracis*, can pass into the CNS, traversing the physiological BBB.

More serious and uniformly lethal (100% of cases) outcome follows frequently with the development of anthrax meningitis and meningo-encephalitis. An incident of accidental aerosol release from a research facility in Sverdlovsk, Russia, in late 1980's showed a potentially terrible risk to a population from these microbes. Some recent events of intentional spread of anthrax spores in small populations by some person(s) in the United States have illustrated a possible, though remote, use of *B. anthracis* as a weapon of bio-terrorism. Although at this time antibiotic therapy against inhalation anthrax can be restorative if administered in the early stages of infection, no effective therapy is available for the late stages of systemic dissemination or CNS invasion.

Government agencies such as National Institute of Allergy and Infectious Diseases, United States Public Health Services and the U.S. military have placed high priority on the development of agents to inhibit the effect of exposure from *B. anthracis*. Most of the post-exposure treatments and research have been targeted on the development of therapeutics for preventing the internalization of the known virulence factors Lethal Factor (LF) and Edema Factor (EF) into the cells in early stages of anthrax.

However, the pathological findings of severe damage to organs and tissues observed at autopsy differ grossly from the limited toxicity and hypoxic liver failure

caused by Lethal Toxin (LeTx). Involvement of some additional virulence and tissue degrading factors in anthrax secretion are obviously indicated, and some recently identified metalloproteases have been suspected to be likely culprits. Earlier studies offered the intriguing possibility of metalloprotease activity causing injury to the endothelial cells of the CNS microvasculature, which might induce permeability of the blood-brain barrier (2). To fully understand the pathogenic mechanism involved in anthrax invasion of the CNS we need to briefly review the epidemiology, and microbiology, in the context of the clinical manifestations of this disease.

Epidemiology

As the soil-based spores are the natural resting form of *Bacillus anthracis*, the primary victims of the disease are grazing animals that get infected by ingesting the spores or harbor the spores on their body. Humans are incidental hosts, acquiring the infection through close contact with or consumption of uncooked meat or infected animal products. The challenge it poses to animal husbandry and veterinary medicine has been evident in massive epizootics of anthrax among herbivores, such as recorded by the Roman poet Virgil from as early as the first century B.C.. As was detailed by the poet in his didactic verses on agriculture, a large epizootic of anthrax that took place in the Roman district of Noricum, in the Danube River delta, caused death of cattle, sheep, horses, and also other domestic and wild animals feeding upon the herbivores. Even more ancient accounts of the disease can be traced in the writings on the famous Plague of Athens in the Greek literature, which was an inhalational anthrax epidemic (3). In fact, the name of Anthrax was derived from the Greek word *anthracites*, which means,

coal-like, in reference to the black eschar typically forming in cutaneous anthrax (4). Throughout the Middle Ages there were sporadic livestock infections with anthrax (3). In modern times, the epizootic in Iran in 1945 that killed a million sheep also points to possible risk to human society (5).

Thus, a primarily zoonotic disease can become an equally dangerous fatal infection in its incidental hosts. Again, in the 19th century England the mill workers working with sheep wool were commonly affected with anthrax; hence, in Victorian England, the disease gained the popular nickname, "Wool sorters' disease". Other names of the disease have been "rag pickers' disease", "tanners' disease", and "Siberian (Splenic) fever" (4).

Although human anthrax infections are reported to occur occasionally and sporadically in agricultural areas in parts of the world, its incidence has become low with the introduction of animal vaccination. Human anthrax can take various forms depending on the route of infection, - inhalational, cutaneous, or gastrointestinal (GI). Although historic cases of natural epidemics were, in most cases, inhalational, most human cases of anthrax these days are commonly cutaneous, with an annual worldwide incidence reported to be about 2000 (4). Between 1945 and 1994, 224 cases of cutaneous anthrax cases were reported in the U.S. (6). The largest quiet epidemic of cutaneous anthrax affecting more than 10,000 humans occurred in Zimbabwe between 1979 and 1985. However, the inhalation route may still remain a possible, though remote, risk for any large-scale human epidemic in the future under some extenuating circumstances that may release dry anthrax spores in localized aerosols. While use of bacterial warfare was

banned by the United Nations (UN) in 1972, *B. anthracis* remains, at least theoretically, a potent agent for bio-terrorism. An incident of anthrax infection in 11 persons in the U.S. in a random fashion in October of 2001, with 5 fatal outcomes, subsequently turned out to be an act of domestic terrorism. On the other hand, the large-scale anthrax epidemic causing about a thousand fatalities that occurred in Sverdlovsk, Russia on April 2, 1979 happened due to accidental release of aerosolized anthrax spores from a microbiology research facility. Unfortunate as these incidents are, they opened our perspective on a lingering risk of anthrax infection in large populations, and underscore the need for more understanding of the disease mechanism and its prevention and treatment.

Microbiology of B. anthracis

As a significant disease agent, the anthrax bacilli drew the attention of some leading experimental biologists in Europe of the latter half of the 19th century. Interestingly, anthrax became the model organism for development of the "Koch Postulate" on infectious disease transmission by Robert Koch in Berlin, Germany. In 1876 Koch followed the complete life cycle of anthrax bacilli using his suspended drop culture technique, and also grew the organism *in vitro* and demonstrated its ability to transmit disease in healthy animals inoculated with material from the culture. Again, in 1881 Louis Pasteur in Paris successfully immunized cattle against a virulent strain of *B. anthracis* with his vaccine preparation containing live attenuated organism, thereby proving his Germ Theory of Disease (7; 8).

B. anthracis is a relatively large, aerobic, gram-positive, spore-forming, and nonmotile bacteria belonging to the *B. cereus* group of the bacilli genus which includes

70 species. Other members of the small group, namely, *B. subtilis, B. thurigiensis, and B. mycoides* are nonvirulent (9). Growing well in a variety of laboratory media at 37° C, *B. anthracis* forms white gray colonies of oval-shaped cells with slightly granular appearance (4). Under unfavorable conditions, e.g., in states of nutrient deprivation in the environment or in a culture medium or infected animal body fluids exposed to ambient oxygen, the bacilli form spores. The spores germinate into vegetative forms when exposed to favorable conditions but survive poorly outside an animal or human host (10). In contrast, anthrax spores can survive for decades in the environment.

Pathogenesis and general clinical manifestation

Infection with anthrax begins with the entry of the spores either in inhaled aerosol, through a break or abrasion in host skin, or through ingested food in the gastrointestinal tract. The full complement of anthrax pathogenesis involves a combination of virulence factors, including, three plasmid-encoded toxin components and an antiphagocytic capsule that resists phagocytosis of the vegetative form of the bacilli (10). The capsule is encoded by the plasmid XO2 (pXO2) (95.3 kilobase pairs) and is composed of a high-molecular weight polypeptide containing poly-D-glutamic acid (11). Plasmid XO1 (pXO1) encodes three toxins, called, edema factor (calmodulin-dependent adenylate cyclase), the 83-kDa lethal factor, and the 85-kDa protective antigen (12-14). Although these individual proteins are nontoxic, they act in binary combinations to produce toxic responses in the host body. The LeTx is a combination of the protective antigen with the lethal factor (15-17). The LeTx is cytolytic for macrophages and causes

the release of tumor necrosis factor and interleukin-1, which in turn cause damage to the endothelial cells (4).

After being phagocytosed by macrophages at the site of entry, the spores germinate into vegetative form and multiply extracellularly and produce toxins namely, LeTx and edema toxin (EdTx). Inhaled anthrax spores (1–2 μm in diameter) initially accumulate in the lung alveolar spaces, from where these are carried to the medistinal lymph nodes via the local lymphatic ducts. Germinating in these nodes, the vegetative bacilli cause hemorrhagic lymphadenopathy, as typically observed in the widening of the mediastinum with effusion on a chest radiograph (4). The initial phase of the infection (prodromal phase) beginning in 2-5 days after exposure with influenza-like symptoms include, mild fever, malaise, fatigue, and a nonproductive cough, which lasts for about 48 hrs. The second phase presents with rapidly developing respiratory distress, e.g., severe dyspnea and stridor, fever, and cyanosis, which are attributed to the pulmonary edema and host inflammatory response with release of tumor necrosis factor and interleukin-1 elicited by large amounts of anthrax toxin. As a result, rapidly developing septicemia can cause death in the untreated patients in a short few days. Antibiotic therapies after the onset of septicemia may not be effective. Studies on inhalational anthrax in experimental monkeys have shown that even with treatment, the residual spores may germinate up to 60 days, causing relapse of morbidity and death; therefore the antibiotic treatment is recommended for 60 days (18).

Cutaneous anthrax infection remains the most common form of human anthrax these days, while the risk of acquiring the disease from inhalation has declined with

improving agricultural and industrial hygiene practices. Anthrax spores entering a skin abrasion germinate in the localized soft tissues with production of toxins and edema. A ring of painless, pruritic vesicles develops on the skin site followed by ulceration of the central papule, which dries to form a black eschar. In many cases the eschar dries and is shed in 1 to 2 weeks (19). Although cutaneous lesions heal with minimal or no treatment in most cases, about 20% of untreated patients develop systemic septicemia with painful lymphadenitis and die, as in inhalational disease described above (20).

Anthrax infection of the gastrointestinal tract may occur through the alimentary mucosa from consumption of uncooked meat of infected or spore-contaminated animals. Affected oropharyngeal areas develop ulcers, regional lymphadenopathy, edema, and sepsis (21; 22). Different parts of the GI tract in the abdominal region, usually, stomach, duodenum, cecum, and terminal colon, can also be involved and develop ulceration and black eschars, associated with edema and lymphadenopathy. Presenting symptoms in abdominal anthrax are nausea, vomiting, anorexia, and fever, progressing to severe abdominal pain, hematemesis, and bloody diarrhea, ending in septicemia and death (4; 10).

Edema and multiorgan hemorrage are hallmarks of anthrax infection, and the distribution of lesions and septicemia are usually identical in all forms of untreated and advanced anthrax, except for the distinguishing marks of entry in the cutaneous and GI tract forms and the mediastinal edema and widening in inhalational anthrax. As the illness advances rapidly, extreme disorientation, rapid and faint pulse, and dyspnea ends in coma and death (23; 24). Involvement of the CNS is an end-stage process.

All three forms of anthrax can develop into meningoencephalitis, but in some series about 50% of the inhalational anthrax patients developed hemorrhagic meningitis (4; 10), and these cases were uniformly fatal. On the contrary, hemorrhagic meningitis should raise suspicion of anthrax infection (25). Less often cutaneous anthrax progresses to meningoencephalitis; however, this form has been found to carry a better prognosis than in inhalation anthrax, with survival of about 5% of patients (26).

It is intriguing that only a few pathogenic microorganisms, including *B. anthracis*, cause most cases of CNS infection although almost all human pathogens have the potential to invade the brain. An answer to this enigma may lie in either or both of the specific structural and functional components of the blood-brain barrier (BBB) and specialized properties of the pathogen. A discussion follows on the molecular components of the BBB that determine or characterize its physiological functions and pathological aberrations thereof.

Blood-retinal barrier (BRB)

In the past, more conventional BBB *in vitro* model cells have been isolated from human tissue samples, obtained from the NIH and other institutions. These primary cultures are called HBMEC (27).

Toimela et al., 2003 (32), suggested that human retinal pigment epithelial cells (ARPE-19) could be used as a novel model for BBB studies. The RPE cells play an important role in the functionality and viability of the eye via and transport of nutrients, maintenance of the BRB for selective permeability, release of factors (e.g., growth

factors/trophic factors) in order to maintain surrounding photoreceptors (28) and phagocytosis of proteins shed from the photoreceptors (29).

Even though ARPE-19 cells are not considered endothelial brain microvascular cells, they still possess the characteristics and function that are similar to the BBB or endothelial cells of the brain (30). One of the most important characteristics is the maintenance of BRB within the eye. Specifically it regulates the exchange of nutrients and metabolite in between the retina and the choriocapillaris (31). These cells are of neural origin (30), are relatively stable in culture, express and retain most of their natural characteristics *in vitro* (32), and are able to form tight junctions when cultured on microporous filters (30).

Blood-brain barrier (BBB)

The physiology of the CNS has a remarkable property of restricting passage of molecular serum components from the general circulation. This functional BBB concept, first proposed by Paul Ehrlich, a German physiologist (1885), is evident from the exclusion of high concentrations of neuroactive amino acids in the systemic blood and also in the difference in the chemical composition between the cerebral spinal fluid (CSF) and blood. Anatomically the BBB has two components: 1) between CNS blood vessel lumens and the extracellular spaces of neuronal cells formed by the capillary endothelial cell lining within the tight junctions of brain blood vessels; and 2) between blood and the subarachnoid space of the CSF, formed by the tight-junctions of the epithelial cells in the choroid plexus (33). The specialized features of these two sites of selective transport can account for the ability of the BBB to help maintain the unique internal milieu of the

brain, and retard the movement of many toxic products, drugs, and pathogens from the general circulation to the brain (Figure 1).

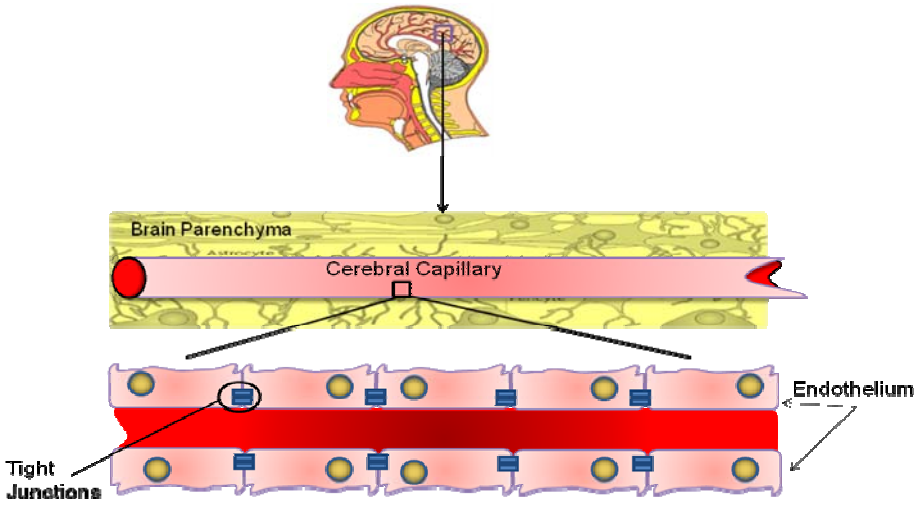

Figure 1. Anatomical model showing components the blood-brain barrier (adapted from (140))

The endothelium of the cerebral vessels is composed of non-fenestrated cells, unlike the peripheral vessels; the tight junctions arise early in development, but as it matures and permeability becomes restricted, specific molecular transport systems for glucose, amino acids, and ions to support neuronal functions also become operational (34).

The sub-arachnoid CSF space, on the other hand, is separated from blood by the tight-junctions of the epithelial cells in the highly vascularized four cerebral ventricles where the CSF is produced by a filtration process analogous to that in the kidney (33). Pathogens or toxins from the blood may enter the CSF along with blood itself, if this selective barrier of polarized epithelia is disrupted in disease or injury. The CSF has

continuous turnover replacing its entire volume in four to six hours. The normal CSF is poor in nutrients such as amino acids and ions, and in buffering capacity, as well as in the immunological components of host defenses such as, complements and leukocytes (44). The more extensive BBB between the brain and the general circulation is defined by the endothelial cells of the cerebral microvasculature; these cells are characterized by the properties of their tight-junctions and sparse pinocytic activity, unlike the endothelia of other peripheral blood vessels.

Tight- junction of the BBB

Tight-junctions (TJs) belong to a group of specialized and highly organized junctional complexes that form the barrier function in epithelial cells and endothelial cells, including, adherens junctions (AJs), gap junctions, and desmosomes. A number of proteins constituents of the junctional complex have been identified including several integral membrane proteins such as claudins, occludins, and cadherins. Also, intimately associated are components of the signaling system, e.g., protein kinases, tyrosine kinases, small G-proteins and the zonulins (ZO-1, ZO-2, and ZO-3) that can function as scaffolding proteins for signaling molecules. This property of the complex networks of TJ strands has been of advantage to my TEER measurements as an index of HBMEC permeability, as predicted years ago by Marcial et al., 1984 (35).

Although most of the TJ studies have been carried out on epithelial cells, convincing evidence for a more complex tight junction existing in the endothelial cells of brain capillaries was presented by Nagy et. al., 1984 (36). Other investigators subsequently revealed some notable differences between epithelial and endothelial tight -

junctions, and also between those of the peripheral organs and those of the CNS capillary endothelia (Blood-brain barrier). A difference of blood-brain endothelial cells is that cadherins stretch along the entire intercellular cleft, in contrast to epithelial cells (37; 38). The tight junction morphology and regulation in both epithelial and endothelial cells have some unique components that determine their barrier characteristics, even though many junctional components are similar (39). These distinctions are critical in the functional differences between the BBB (endothelial) and the blood-cerebrospinal fluid barrier (epithelial).

Morphology, molecular development & maturation

The microstructures and topography of the TJs have been studied in ultra-thin sections and freeze-fracture electron microscopy techniques revealing that epithelial TJs are associated predominantly with the protoplasmic fractures (P-face) forming a network of strands, while the grooves of the external fracture face (E-face) carry very few particles. The particles on the E-face are arranged in chains, but the P-face particles, more commonly in the epithelia, form smooth, continuous cylindrical profiles. The discontinuous and irregular appearance of TJ particles on the E-face are likely to be due to multiple linkage sites of protein complexes to the cytoskeleton (40; 41). Presumably the smooth continuous strands on the P-face may represent a lipid meta-structure.

Interestingly, the TJ of the endothelial cells of the leaky peripheral vasculature has less complex network containing anastomosing strands and many open ends (42; 39; 43). Further, in peripheral endothelium the TJ particles are predominantly associated with the E-face, in contrast to their higher association with the P-face in BBB (55%

versus approximately 10%) on the P-face of the peripheral endothelial cells. The topography of the TJ components thus appears to be a major determinant of maintaining the vertebrate BBB. Early embryonic brain capillaries are not fully equipped to maintain the BBB, and are still permeable to substances that are excluded from the neuronal milieu in the adult. The TJ particles' association in the cerebral capillaries has been found to undergo alterations in rat brain during development; from a predominant E-face during E15 and E18 embryonic days to predominantly P-face association in postpartum day 1 (P1) and adult rats. Also for human embryos a high degree of E-face association has been documented (44).

The specialized structures of the BBB endothelia serves to maintain the selective barrier function for nutrients and humoral transmission as well as regulatory and signal mediating functions. Whereas gap junctions mediate intercellular communications, the AJs and TJs act to restrict permeability across the endothelial cadherin, a calcium-regulated protein mediating cell-cell adhesion (45). Given that AJs disruption can cause increased BBB permeability, it is the TJ that primarily confers the low paracellular permeability and high electrical resistance (46).

Several transmembrane components of TJ at the BBB have been identified and characterized, e.g., JAM-1, occludins, and claudins. JAM-1, a 40 kDa protein of the IgG superfamily, is believed to mediate the early attachment of adjacent cell membranes by homophilic interactions (47). JAM-2 and JAM-3 are present in endothelia but not in epithelial cells. In addition to their developmental roles, JAM proteins may have some

regulatory role in trans-endothelial leukocyte migration, but their function in mature BBB is still uncertain.

TJ stands are composed mostly of (20 iso-types) claudins. Occludin is a transmembrane protein, 60 to 65 kDa, which gets incorporated into the claudin polymers. Occludin increases TEER in TJ-containing tissues, and the protein has multiple serine and threonine residues as phosphorylation sites. Occludin may associate with the cytoskeleton in conjunction with accessory proteins like Zonulin -1 and 2 (48-50). However, several knock-out and knock-down studies have shown that occludin is not essential for the formation of TJ, although it has been found that in several disease states, a decrease in expression of occludin is associated with disruption of BBB function. Conversely, expression of occludin does not lead to the formation of TJ. Several investigators have hypothesized that claudins form the primary seal of the TJs, and occludin acts as an additional support structure (48-50). These molecular interactions between components of the BBB can be seen in Figure 3.

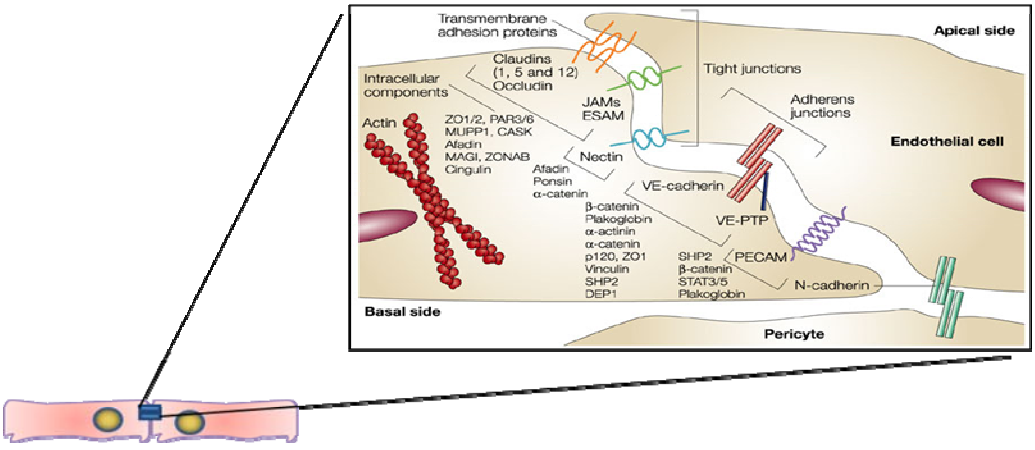

Figure 2. Endothelial cell TJs (adapted from (51)).
Representative model of junctional proteins between endothelial cells.

The first protein identified in the TJ was a 220-kDa protein named zonulin (ZO-1). It is a phosphoprotein expressed in endothelial and epithelial cells, as well as in many other cells that do not have TJ (52; 53). ZO-1, ZO-2 and ZO-3 have been considered as belonging to a group of accessory proteins that associate with the TJ components in the cytoplasm and have properties like the membrane-associated enzyme guanylate kinase.

Hence, these proteins have been identified as membrane-associated guanylate kinase-like homolog family (MAGUK). Guanylate kinases are enzymes catalyzing the ATP-dependent conversion of GMP to GDP. However, the homologous sites for binding of ATP or GMP are lacking in some of these MAGUK proteins, thus rendering them enzymatically inactive (54).

ZO-1 is a membrane-associated guanylate kinase-like protein. ZO-1 has been found in TJ and also in AJ and gap junction, but there is no TJ without ZO-1. ZO-1 connects the other transmembrane proteins of the TJ to the actin cytoskeleton and to occludin, and this supports the stability and function of the TJ. It functions in organizing and clustering of protein complexes to the cell membrane which plays an important role in establishing specialized domains in the membrane complexes, as seen in Figure 3 (55). This key functional role of ZO-1 gains support from the observation that its disruption causes increased permeability (56). ZO-1 has several isoforms due to splice variations. Two of these variants, α^+ and α^- were thought to be characteristic for epithelial or endothelial TJ respectively (57; 39). This characterization was based on their relationship to junctional plasticity, with the α^- variant expressions in structurally dynamic TJs, as occurring in endothelial cells. Moreover, molecular interactions between

these junction complexes to actin are important to the structural integrity and function of tight junctions. The major protein domains of ZO-1 include PDZ, SH3, GUK, and C-terminal domains. PDZ domains comprise 3 separate PDZ modules (e.g., PDZ1, PDZ2 and PDZ3), which serve as scaffolding, binding, and spatial clustering of transmembrane proteins. The PDZ1 domain binds claudin proteins, integral tight junction proteins of the BBB; the PDZ2 domain anchors other zonnulin proteins such as ZO-2, and ZO-3. SH3 (src homology 3) is involved in binding phosphoproteins and Y-box transcription factor ZONAB, which regulates paracellular permeability and cell cycle. The guanylate kinase domain of ZO-1, modulates protein-protein interactions between occludin proteins, thus playing a major role in BBB barrier integrity and organization. The C-terminal end of ZO-1, which is defined by acidic and proline-rich regions, binds cytoskeleton proteins, e.g., actin, which is important in maintaining cell shape and motility and plays a critical role in modulating BBB permeability (55). Therefore, ZO-1 is recognized as a modulator of BBB integrity and permeability.

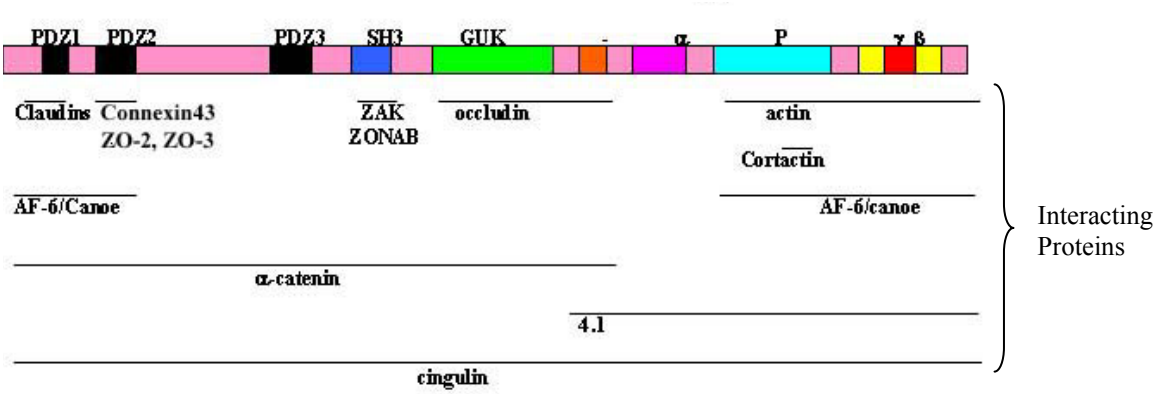

Figure 3. ZO-1 domains and binding partners (adapted from (55)).
ZO-1 protein is part of the membrane associated guanylate kinases (MAGUK) family. MAGUK have a number of domains that regulate protein-protein interactions including: PDZ domains, an SH3 domain, and an enzymatically inactive guanylate kinase domain (GUK). As shown in the figure, ZO-1 binds to a large number of different proteins (interacting proteins) that are found at cell-cell junctions.

ZO-2, a 160 kDa phospho-protein, co-precipitates with ZO-1 with which it has high sequence homology. Although less is known about the sparsely distributed ZO-2, it binds, like ZO-1, to both structural components of TJ and signaling molecules, e.g., transcription factors (58), and localizes into the nucleus during stress and proliferation (59; 60). ZO-2 distribution in cultured brain microvasular endothelial cells is mainly localized along the cell-cell contact sites of the membrane. In cultured epithelia lacking ZO-1, it is possible that ZO-2 has an auxillary role in the formation of morphologically normal TJ. As said for ZO-1 above, some non-TJ tissues also have been found to contain ZO-2 (61). ZO-3 (130 kDa protein) is another variant of ZO, found in some TJ-containing tissues, but not at the BBB (62).

Additional proteins with accessory functions

The TJ forms the most apical component of intercellular juncitonal complexes; it separates the apical from the baso-lateral cell surface domain (63). This serves a "fence function" by maintaining polarity, as well as the "barrier function". The fence function works at the subcellular level, while the barrier function (gate) works at the organ level. As mentioned above, the TJ of the BBB has not only to maintain selective permeability of ions and essential nutrients, but also to control passage of neurohormones and needed growth factors and hormonal signals. Thus, interactions between the TJ and the cytoskeleton for signal transduction involves other accessory proteins, such as cingulin, a 140 to 160 kDa protein that interacts with ZOs, JAM-1, and myosin (64; 46). It has been observed that interaction of ZO-1 with AF-6, a 180 kDa protein carrying two Ras-associating domains has a reverse relationship with Ras activation. Activation of Ras is associated with loss of ZO-1 from the junctional complex and an increase in permeability. This suggests, modulation of TJ by ZO-1/AF-6 complex may be linked with Ras pathways (65). It is becoming clear how signaling components and active molecules interact with TJ in determining the BBB structure and function in response to various stimuli.

Second messenger pathways involved in TJ function

G-Proteins

Heteromeric G-proteins are expressed by cerebral endothelial cells where they mediate migration of T-lympocytes (66; 67). G-proteins were found to be involved in the development and modulation of TJ (57; 68; 69).

Phosphorylation

Both transmembrane and accessory proteins of TJ have been found to undergo post-translational modification by phosphorylation, which may be part of the major regulatory processes. For example, claudin-5 at the junction in cultured brain endothelial cells show increased immunoreactivity in the presence of added cAMP. Also, subcellular localization of occludin is subject to regulation by phosphorylation of its serine residues (70). In fact, some early studies suggested that the degree of phosphorylation of ZO-1 correlated with its targeting during development (71) and also that junctional permeability correlated with ZO-1 phosphate content (72). However it has not yet been possible to correlate these phosphorylation states with any of the regulatory processes in these cells; it seems unlikely in light of the findings that multiple TJ proteins get phosphorylated, including both ZO-1 and occludin (73).

Calcium

Calcium dynamics across cell membranes are now a well-known mechanism of signaling and cell activation. It was found quite early for TJ that depletion of extracellular Ca^{2+} and /or increased intracellular Ca^{2+} could cause disruption of BBB (74). Epithelial cells have been observed to lose ZO-1, ZO-2, and occludin with increased paracellular permeability when cultured in a Ca^{2+}-deficient medium (75). The evidence on overcoming of the deleterious effects of Ca^{2+} deficiency when protein kinase C (PKC) is activated suggests that PKC has a role in Ca^{2+}-dependent regulation of TJ (57). Moreover, Ca^{2+} influx or release from intracellular stores also can activate many kinase enzymes of the signaling cascade and activate several transcription factors that regulate

TJ protein expression (e.g., mitogen-activated protein kinase/MAPK, c-fos, c-Jun, nuclear factor κB, cAMP response element binding protein, etc.); however, any role of intracellular Ca^{2+} rise on the MAGUK proteins is still uncertain (76; 46).

Tight junction in BBB dysfunction and disease

Given our current understanding of the structure and functional roles of the TJ proteins in maintaining the BBB, their dysfunction may contribute to several CNS diseases. Even though accurate correlation in all conditions cannot be determined in our present knowledge of the intermolecular regulation, the development and progression of several neurological diseases are related to failure of the BBB. The major reasons for the incomplete understanding remain, absence of appropriate animal models, and a multitude of intrinsic and extrinsic influences on the CNS functions that cannot be viewed in any simplified system. Understandably, chronic hypertension can cause stress and impairment of the vascular endothelium. Subtle barrier impairment in the BBB of healthy but stroke-prone rats has been observed, which has been associated with an increased ratio of the E-face/P-face distribution of TJ particles (77). Finding no alterations in the immunoreactivity of TJ proteins or in the capillary permeability, the authors have proposed the hypothesis that a rearrangement of the cytoskeletal coupling of the TJ proteins might have been responsible for the altered E-face/P-face associations. Increased neuro-vascular permeability has also been noted in diabetes, a chronic disease with microvascular effects, with known risk for ischemic stroke (78). Barrier breakdown is known to occur in other chronic neurological diseases, e.g., multiple sclerosis (79-81). Short-term CNS insults, e.g., hypoxic injury and drug abuse also have been found to

compromise BBB function and brain edema (46). Interestingly, a reorganization of the BBB TJ seems to be partly mediated by vascular endothelial growth factor (VEGF) and its mediator nitric oxide (82; 83).

Tumorigenesis, the most devastating progressive disease of CNS has been followed for associated change in the BBB TJ. Early investigators on brain tumors recorded a complete breakdown of BBB, associated with peritumoral edema (84; 81). Another strong indicator of tumor correlation with TJ was, a finding that down-regulation of ZO-1 expression was coupled to cancer progression (85). Interestingly again, it was observed that in Drosophila, the deletion of the Disc-large tumor suppressor (*Dlg*) gene which encodes a guanylate kinase homolog (recall MAGUK proteins of TJ) produces a neoplastic phenotype (86).

From the above review on the arrangements and inter-relationships of TJ proteins including zonulins, we gather a comprehensive glimpse of the delicately tuned functions of the BBB in its role of barrier and fence functions, as well as in diverse physiological signaling mechanisms. Naturally, then it follows that many developing pathologies of the CNS may also be causally linked to a critical disturbance in this finely tuned system. Our research into anthrax meningitis has been guided by this understanding of the BBB, and therefore, focused on the fate of the endothelial TJ components.

Possible pathways for pathogens to access through the BBB

The structural and functional characteristics of the TJ in both endothelia and epithelia of the BBB suggest that this may be the target for blood-borne bacteria to attack and gain access into the CSF space, or into the brain parenchyma.

Theoretically, microbes or hematogenous toxins can gain access to the brain intercellular space by overcoming the BBB via four possible mechanisms: 1) direct penetration of the TJ of the choroid plexus to enter into the CSF, causing meningitis; 2) by disrupting the barrier function and circumventing TJs of cerebral capillary endothelium, thereby gaining access into the brain parenchyma. This results in encephalitis; 3) of the capillary endothelium; and 4) a so-called "Trojan Horse" mechanism involving migration on or within phagocytes. The process, resulting in transcellular migration of the endothelium, involves enhanced adherence of the pathogen to certain molecules on the post-capillary venules for transmigration. This occurs with cerebral malaria which targets a cell adhesion molecule ICAM-1 (87). Some prolonged low-grade bacteremia, caused by pathogens such as *Listeria, Treponema*, *Rickettsia*, and *Plasmodium*, or sustained high-grade bacteremia can invade the BBB by this mechanism (33). However, high-grade bacteremia leading to meningitis suggests the choroid plexus as the site of entry, whereas prolonged, low-grade bacteremia, often causing multifocal encephalitis (attacking the brain parenchyma) points to crossing the endothelial BBB. Entry into CSF can occur by the choroid plexus epithelium or can occur by penetration of larger cerebral vessels or at the subarachnoid granulations. CSF is continuous with the extracellular fluid; yet an early phase of meningitis usually spares the parenchyma.

Paracellular transmission indicates a functional disturbance in the TJs that can allow even low-grade bacteremia to filter into the CNS. Such functional alterations in the TJs can result at any of the sites through glial cells, basement membrane, adjacent zonula adherens, and by circulating cytokines. The zonula adherens contains several

macromolecules such as cadherins, catenins, actin, and other proteins. Although high concentrations of cytokines during sepsis have not been found to induce leaky TJs (33), a saturable transport system for IL-1α and IL-1β has been associated with enhanced BBB permeability (88).

Transmigration, by carriage within or on macrophages, although theoretically possible and has been observed with one pathogen *Streptococcus suis* type-2, carried within leukocytes found within the CSF, is extremely rare in pathological records (33).

Clinical case studies of several sources of infectious meningitis offer glimpses of BBB invasion of pathogens by mechanisms that utilize some molecular components of the BBB itself. Examples include, engaging the receptors for platelet activating factors (PAF) by pneumococci (89), production of bacterial proteins that mimic BBB endothelial molecules important for promoting trafficking of leukocytes, or production of protease with specificity against BBB endothelial TJ proteins, such as *Pseudomonas* Elastase which specifically degrades ZO-1 protein (89). Investigating the interactions of the bacterial components with BBB components should help us understand not only how BBB permeability is achieved in the process of pathogenesis, but also the unique properties of the BBB to which new therapies can be directed.

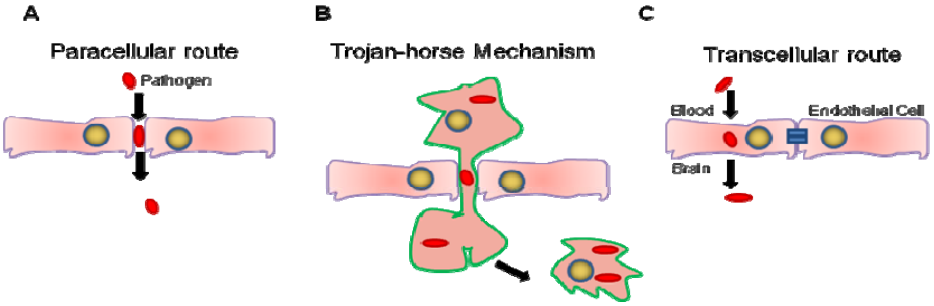

Figure 4. Mechanism of microbial invasion through the blood-brain barrier (adapted from (140)).
(A) Paracellular traversal, pathogens cross the BBB between cells with or without the destruction of tight-junction proteins. (B) Trojan-horse mechanism, pathogens infect macrophages and then traverse the BBB. (C) Transcellular route, microbes cross the BBB by receptor-mediated endocytosis or physically penetrating endothelial membrane.

2. STUDY OBJECTIVES AND OUTLINE

Our research focuses on the pathogenic mechanism of *B. anthracis* in CNS injuries accompanied by meningo-encephalitis. Given the fact that the CNS is largely protected by the BBB, it remains intriguing how *B. anthracis* circumvents this protective barrier and gains access to the CNS parenchyma. In searching for the site and mechanism of the anthrax toxin's attack on the BBB, our attention is drawn to the endothelial components forming the TJs. Earlier studies in our laboratory have yielded results that secreted anthrax protease degrade extracellular matrix proteins and blood proteins involved in hemostasis and thrombosis. Our pilot experiments showed that the TJ protein, ZO-1 is a potentially important target for the anthrax-secreted protease. On the otherhand, previous studies in other laboratories had also shown that ZO-1 dissociation from the junctional complexes increases barrier permeability (90).

Anthrax hemorrhagic meningoencephalitis

Bacterial meningitis is a serious infection of the CNS that in most cases ends in fatality or serious neurological deficits in the survivors. CNS infections continue to be an important cause of high mortality and morbidity throughout the world, even in this post-antibiotic era (91). Amongst the most severe pathogenic agents for the CNS, *B. anthracis* is remarkable as a cause of hemorrhagic meningitis with fatal outcome.

Anthrax meningitis can develop from hematogenous spread to the nervous system via inhalational, gastro-intestinal, and cutaneous routes of infection (91). Under normal health conditions, however, access of pathogens or a large variety of macromolecular drugs to the CNS is restricted by the anatomic and physiological BBB. Pathogen invasion of the CNS parenchyma must somehow bypass the BBB through the few anatomic interruptions via a transcellular mechanism, or by disrupting the capillary endothelial lining that forms the BBB. Toxigenic bacteria such as *B. anthracis*, equipped with exotoxins can exert widespread destructive effects on the BBB that are only beginning to be understood.

It remains uncertain whether *B. anthracis* bacteria gain access at all to the CNS, and if so, then how the active, vegetative bacteria may traverse the BBB. Presumably, identification and characterization of toxigenic products or the virulence factors of the pathogens should provide us with the key to understanding the process that disrupts or diffuses through the BBB (paracellular invasion). The known virulence determinants of *B. anthracis* are encoded by two large plasmids XO1 and XO2; and the 2 major virulence factors, a tripartite toxin comprising of the protective antigen (PA), LeTx, and EdTx (located on pXO1) and the antiphagocytic glutamic acid capsule (genes located on pXO2). Earlier studies directed at these virulence factors have considered the LeTx is secreted by proliferating anthrax bacilli to be the major causal agent for patient death. The secreted protein LeTx appears in the circulation of the infected animal in the septicemic stage, shortly before death (92; 93) and thus, has been considered the major late virulence factor, and cause of death.

Pathological studies with experimental animals inoculated with LeTx have revealed drastically different systemic effects than the predictable course of natural infections. The absence of any gross pathologic change in anthrax-infected animals, other than a gross hypoxic liver failure (94) was confirmed in extensive autopsy analysis of mice and rats challenged with highly purified LeTx. While systemic toxicity of LeTx is found to be low, its role in immuno-suppression within alveolar macrophages in the early stages of inhalation anthrax strongly suggests its important role as a disease-establishing virulence factor. This property of LeTx, albeit limited, helps the anthrax spores to survive against host inflammatory reactions. Hence, it has been hypothesized that the main function of LeTx and EdTx might be to create and support a favorable condition for intraphagocytic survival of the bacilli (15; 95-98). This hypothesis also has led to an alternative possibility of the pathogen's disruption of the BBB through a so-called "Trojan Horse" mechanism, by the passage of bacilli-laden macrophages.

Previous studies on the effect of LeTx on human lung microvascular endothelial cells have shown barrier dysfunction with increased vascular permeability (99). Although the toxin components (LeTx and EdTx) are considered as the major virulence factors of the *B. anthracis*, their observed effects cannot fully account for several pathological findings of anthrax, such as massive hemorrhages and intensive organ and tissue damage. Additionally, studies with EdTx-infected mice did not show significant lesions in the liver or brain meninges, indicating the involvement of other virulence factors (100; 101). While the net effects of the LeTx and EdTx are still poorly understood, the evidence suggests their actions may be limited to disease establishing

actions. The massive tissue damage and other pathological consequences including degradation of cytokines and immunoglobulins observed in mice treated *in vivo* with culture filtrates of *B. anthracis* (2) suggest extensive proteolytic activity which may be associated with the bacterial products. It is important to consider the possibility that some anthrax protease(s) may exert a critical pathogenic role.

Previously reported pathological observations on fatal cases of inhalational anthrax may provide important guidelines to the mechanism of disease progression and its outcome. Autopsy findings of this lethal form of infection with *B. anthracis* have shown extensive tissue damage including multiple hemorrhagic lesions in the mediastinum, mediastinal lymph nodes, bronchi, lungs, heart, central nervous system, and visceral organs, e.g., kidneys, liver, spleen, adrenal glands, and the intestines. Widespread vasculitis with diffuse extravasation in moderate-sized arteries to microvessels have accompanied massive necrosis in some tissues (102-104). Particularly intriguing are the hemorrhagic changes in the CNS, which indicates a disruption of the physiological BBB.

Anthrax meningitis usually results from systemic hematogenous spread of *B. anthracis*, which can end in subarachnoid and intracerebral hemorrhage. This theory is supported by gross pathologies found at autopsy examination of patients who developed cutaneous and or inhalation anthrax (26). In cases of accidental exposures to inhalational anthrax in industrial or bioweaponry establishments, up to half of the victims have developed meningoencephalitis (26).

These observations offered an appropriate context to evaluate the causal role of LeTx in patient death, as some early authors considered LeTx to be the major late virulence factor and cause of death (105; 106). While such emphasis on LeTx as the only anthrax protein exerting toxic effects in experimental animals might have diverted investigators' attention from additional or alternative virulence factors, a low systemic toxicity from LeTx was also noted (107; 106). Moreover, clinical manifestations of systemic anthrax infection, including widespread vascular leakage, hemorrhage, and shock are different from the histopathologic findings that gross changes of LeTx intoxication are generally limited to hypoxic liver failure (108; 94).

The earlier assumption that the gross pathology is caused entirely by LeTx contained in the culture filtrates of *B. anthracis* was recently questioned. The gross systemic injuries and diffuse hemorrhage observed in autopsy studies accompanied by other clinical-pathological findings of degradation of inflammatory mediators and immunoglobulins point to the possible involvement of other tissue-damaging enzymes, virulence factors, or activators of host body's proteolytic enzymes in the destructive processes.

Interestingly, other authors have found a variety of potential virulence enhancing factors by analysis of the chromosome sequence of the nonpathogenic *B. anthracis* Ames strain. These include phospholipases, collagenases, hemolysins, and other enterotoxins containing sequence homology with similar products in other pathogenic species (109). Popov et al., (2), have drawn our attention to a group of proteases encoded on the *B. anthracis* chromosome, which are shared in common with its pathogenic group

representative, *B. cereus*, but absent in the genomes of nonpathogenic members of the group, such as *B. subtilis* and *B. halodurans*. These include several proteases, such as, thermolysin-like metalloproteases of the M4 family, which are capable of causing massive internal hemorrhage and life-threatening pathologies (110-114). Using these M4 family proteases carrying hemorrhagic, caseinolytic, and collagenolytic properties along with M9 thermolysin and bacterial collagenase family metalloproteases, researchers have demonstrated their direct *in vivo* toxicity by injecting them into DBA/2 mice. Further, the tissue destructive action of these proteases was confirmed by observing substantial protective efficacy of chemical protease inhibitors, as well as anti-M4 and anti-M9 immune sera. In addition, the improved protection efficacy of these antidotes administered against anthrax spore challenge in combination of the antibiotic ciprofloxacin, 48 h post-exposure (compared to ciprofloxacin alone) strongly suggested a critical role of *B. anthracis* metalloproteases in causing serious tissue injuries.

In addition to the biochemical properties of metalloproteases, a comparative proteomic analysis of *B. anthracis* indicates these proteases are also expressed in natural biological conditions after an anthrax infection, suggesting their biological relevance (115). Such proteases may include neutral protease 599 (Npr599) and immune inhibitor A metalloprotease (InhA). Npr599 is a thermolysin-like enzyme homologous to bacillolysins from other *Bacillus* species, and immune inhibitor A is an enzyme homologous to InhA of *B. thuringiensis*. These proteases belong to the M4 and M6 families, respectively. Both enzymes digested various substrates, including extracellular matrix proteins, endogenous inhibitors, and coagulation proteins (100). Although this

finding does not prove proteases to be virulent, it is one of the qualifications to be a potential virulence factor in anthrax infection.

This research was undertaken to explore the mechanism of CNS invasion and pathogenic action of *B. anthracis*. Therefore, studies were conducted on the identification of the causal agent and characterization of the mechanism of action(s) that can disrupt or overcome the normal restriction of the BBB. The bacterial proteases mentioned above drew our special attention not only because of their tissue destructive potential, but also as possible mediators of pathological changes in the BBB resulting from anthrax infection.

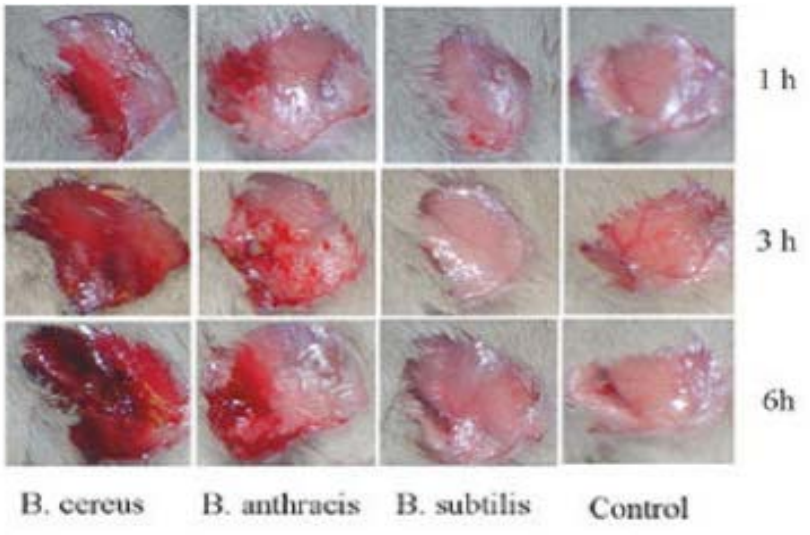

Figure 5. Hemorrhagic activity of culture supernatants.
100 µl of secreted proteins (20 to 100 µg) were subcutaneously (sc) injected into the femoral artery region for observation of hemorrhagic changes. The fur over the femoral artery region was removed to allow observation of a 1.5 to 2.5 cm2 area of skin. Control mice were administered equal amount of phosphate-buffered saline (2).

Central hypothesis

Our early physical and morphological studies comparing effects of InhA and Npr599, as illustrated in the results (Figures 7 and 8) showed that only InhA produced changes on HBMEC. That observation led us to hypothesize that anthrax-secreted protease (InhA) might bind to the cell surface on microvascular endothelial cells of the human brain, and directly exert its proteolytic activity, or alternately, might be internalized, to induce degradation of TJ protein ZO-1. If the former effect would happen, then meningitis would be inevitably associated with all anthrax infections. On the other hand, the process of InhA internalization seems more plausible, since endothelial permeability depends so much on the TJ proteins, and it turned out in our studies that ZO-1 is the prime target for this protease. My present studies were guided by this central hypothesis. Some recent publications (2) also presented data that support this hypothesis (Figure 5). It has been discussed above that the degradation of ZO-1 leads to BBB dysfunction. Researchers have suggested that *Citrobacter freundii*, a microbe which causes neonatal meningitis, is known to enter BBB and replicate in the brain parenchyma (116). It was also shown that replication and invasion of this bacterium into the BBB or HBMEC are dependent on microfilaments, microtubules, and endosome acidification. The results of this study, coupled with our initial findings on ZO-1 lysis prompted us to examine whether the effects of InhA might also involve a phagocytic-endocytic process. We examined this possibility using phagocytosis inhibitor, Cytochalasin D, which acts on and stabilizes microfilaments. Direct cleavage of ZO-1 in naïve HBMEC lysate by InhA and inhibition of InhA-induced degradation by

cytochalasin D, suggests that InhA could gain access into HBMEC by phagocytic-endocytic process, as illustrated in the model below (Figure 6).

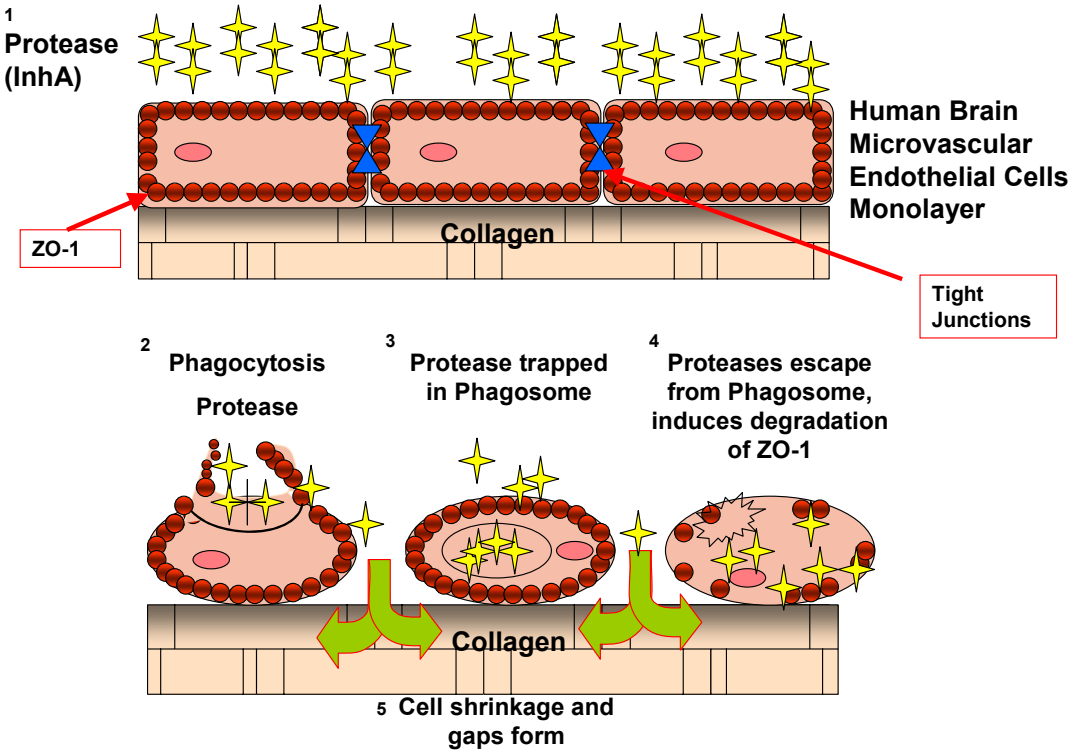

Figure 6. Hypothetical mechanism of ZO-1 degradation in HBMEC.
InhA attaches to cell surface, gets endocytosed, escapes endosome, and induces ZO-1 degradation.

Study objectives

The major objective of this study is to investigate how *B. anthracis* is able to establish CNS infection and cause hemorrhagic meningitis and to understand how the secreted protease InhA from *B. anthracis* can induce BBB permeability. Within the last 10 years, bovine, murine and human brain microvasculature cells have been successfully grown in culture and used to dissect the pathogenic mechanisms of the CNS infection *in*

vitro (117; 118). Our pilot studies using model endothelial cells (HBMEC), suggested a possible target site of the metalloprotease InhA in inducing BBB permeability via several adheren-junction proteins and the TJ protein ZO-1

The overall objectives for this research have been four-fold: 1) to determine the role of the secreted protease (e.g., InhA) of *B. anthracis* in barrier permeability; 2) to identify the molecular mechanism of BBB breakdown by secreted protease InhA; 3) to identify and characterize the molecular target(s) for anthrax-secreted InhA in HBMEC cells and; 4) to confirm observed InhA-induced changes in BBB permeability in the HBMEC and in anthrax murine models. The proposed research has given us insight into whether secreted proteases of *B. anthracis*, as plausible virulence factors, are involved in the induction and establishment of CNS infection.

3. MATERIALS AND METHODS

Endothelial cell culture (HBMEC)

Isolation and characterization of HBMEC were described previously in Stins et al, (118). Briefly, frozen stock of HBMEC between passages 8 and 24 was thawed and then grown in RPMI 1640 medium containing 10% Nu-Serum (vol/vol) (Becton Dickinson, Bedford, MA), 10% heat-inactivated fetal bovine serum (vol/vol), 1 mM glutamine, 1 mM sodium pyruvate, 100 U/ml penicillin-streptomycin, 1% MEM non-essential amino acids, 1% MEM-vitamins in 75-cm^2 flasks at 37 °C in a humid atmosphere of 5% CO_2 and 95% air until confluence. During experiments, the original culture medium was replaced with Experimental Media (XM) containing 1:1 ratio of Medium 199 and Ham's F-12 media (Cellgro, Manassas, VA), 5 % heat-inactivated FBS, and 1mM glutamine.

Epithelial cell culture (ARPE-19)

ARPE-19 cells are retinal pigment epithelia obtained from a 19 year-old female named Amy who died in a car accident. The cell line was obtained from ATCC (Catalog No. CRL-2302; Manassas, VA). Cells were grown in 75-cm^2 flasks at 37 °C in a humid incubator with 5% CO_2 and 95% air until confluence. Propagation media consisted of a one to one ratio of DMEM:F12 Medium (Catalog No. 30-2006) including 10% heat-

inactivated FBS (vol/vol), and 100 U/ml penicillin-streptomycin. All experiments were conducted using cells with no more than 25 passages.

Bacterial strain, growth conditions and preparation of culture supernatant

The non-encapsulated and non-toxigenic strain *B. anthracis* delta (Δ) Sterne [$pXO1^-$, $pXO2^-$] was provided by the by the National Center for Biodefense and Infectious Diseases (George Mason University, Manassas, VA, USA) (119). Verification for plasmid deletion in Δ Sterne stain was established by PCR analysis using primer specific to pXO1 and pXO2. One liter of LB medium was inoculated with 50 ml of Δ Sterne seed culture and vigorously agitated for 30 h at 37 °C to reach stationary phase. Culture was centrifuged at 17,000 x *g* for 30 min at 4ºC. Supernatant was passed through cellulose acetate filter (0.22 μm) to eliminate bacterial spores and vegetative cell and refrigerated at 4ºC until protein purification (100).

Protease isolation, purification and proteolytic activity

Purification, isolation and enzyme activity of proteases (Npr599 and InhA) from culture supernatant of *B. anthracis* Δ Sterne were performed according to procedures in Chung et al., 2006 (100) . Finely granulated ammonium sulfate (Catalog No. BP212-212; Sigma), was added to culture supernatant to precipitate proteins in LB media. The culture supernatant was centrifuged for 20 min at 17,000 X g. The precipitant was reconstituted and dialyzed against Tris-HCl (pH 7.6) buffer with 3 mM sodium azide. DEAE-cellulose (GE Life Sciences, Piscataway, NJ) (bed volume of 60 ml) anion exchange chromatography and elution was completed on the dialyzed protein using a

gradient of 0 to 500 mM concentration of NaCl in 50 mM Tris-HCl buffer. Two major protein fractions were collected; flow through fraction Npr599 and 200 mM NaCl- eluted fraction InhA. Fractions were run on Sephacryl S-200 gel filtration column (Catologue no. 17-0612-01; GE Life Sciences, Piscataway, NJ) with 20 mM Tris-HCl (pH 7.6), elution of the protein fraction were performed with 150 mM NaCl at flow rate of 1.3 ml/min on the HPLC. Fractions (5 ml) were collected, and protease activity was assayed. Active protease fractions were collected and ran on UNO S-1 ion exchange column (bed volume 1.3 ml) (Catalog No. 720-0021; BioRad, Hercules, CA) at a flow rate of 1 ml/min on the HPLC. Elution of protein fractions was done using a gradient of 0 to 1000 mM NaCl in 50 mM Tris-HCl (pH 7.6). All purification procedures were carried out at 4º C. Protease activity was determined by EnzChek gelatinase/collagenase kit for gelatin hydrolytic activity as described in manufacturer's recommended protocols (Catalog No. 53004; Molecular Probes).

Protease assay

Protease activity was assayed during purification using an EnzChek gelatinase/collagenase kit for gelatin hydrolytic activity, according to the manufacturer's recommendation (Molecular Probes). Total of 5 µl of purified protein fractions in 45 µl of digestion buffer (100 mM Tris-HCl (pH 8.0), 0.1% Triton X-100, 5 mM EDTA, and 1 mM phenylmethylsulfonyl fluoride) were mixed with 50 µl of fluorescein-labeled substrate, and then fluorescence intensity was measured after a 1h incubation at 37 °C at 485 nm excitation and 510 nm emission wavelengths. One unit of protease activity was

defined as the amount of protease required to liberate 1 μmol of L-leucine equivalents from collagen in 5h at 37 ºC, pH 7.5. Enzyme activity determined by a standard curve using a collagenase from *Clostridium hystolyticum* (100).

SDS-PAGE and determination of protein concentration

Proteins were separated by Tris/glycine/SDS-PAGE using 4-20% gels under reduced and denaturing conditions. The gels were stained using Coomassie Brilliant Blue R-250 (Catalog No. 20278; Pierce, Rockford, IL) and then destained. Fractions were then combined based on purity of the protein. Protein concentration was determined colorimetrically using the protein assay (Catalog No. 500-006; Bio-Rad, Hercules, CA) dye reagent and the bovine serum albumin (100).

Real-time trans-endothelial/epithelial electrical resistance (TEER) measurements

To pursue the objective of understanding the role of the anthrax-secreted protease in CNS pathogenesis, we determined its potential effects and ability to alter permeability of a model endothelial cell layer using TEER. TEER is a physical measure of how much electrical current passes through the cell monolayer at any point of time. The apparatus measures the amount of electrical resistance the cellular monolayer produces after treatment with the secreted protease InhA. The electric cell–substrate impedance sensing (ECIS) system was used to measure and monitor TEER in ARPE-19 cells and HBMEC, which were used to calculate the integrity of both cell monolayers. In our study, HBMEC were grown on gold-coated film electrodes in microelectrodes 8-well arrays which were purchased from Applied BioPhysics (Troy, NY). Each electrode array

consisted of eight wells with 0.4 ml of culture medium per well. The electrode arrays were attached to a phase-sensitive lock-in amplifier. The voltage between the small electrode and the large counter electrode in each well was monitored by a lock-in amplifier, stored, and processed by computer-controlled instrumentation ECIS (Applied Biophysics, Troy, NY). The wells of electrode array were coated in rat tail collagen (BD Bioscience), 50 µg/ml, prior to being wetted by culture media. HBMEC were seeded at 5 x 10^4 cells per well and allowed to grow to confluence. At cell confluence, the culture media were replaced with XM and allowed to equilibrate for 2 h within the ECIS setup prior to adding InhA and Npr599. InhA (1 µg/ml) or Npr599 (1 µg/ml) was added to the apical aspect of cells in the 8-well cell culture arrays. The resistance of each well was measured at 2 min intervals for 24 h. After 24 h, morphological changes of the HBMEC cell monolayer were observed via differential interference contrast microscopy (Nikon) (120).

Inhibition studies

HBMEC were pretreated with experimental media containing the indicated concentration of inhibitor. The inhibitors were kept throughout the experiment. For cytochalasin D (Catalog No. C2618; Sigma), cells were pretreated for 1 h at 4ºC and then 37 ºC for 30 min prior to treatment with different concentrations of InhA. For inhibition of clathrin-coated pit formation, HBMEC were treated with monodansylcadaverine (MDC, Catalog No. D4008; Sigma) for 30 min at 37ºC before adding InhA. Control cells were treated with an equivalent amount of solvent without the active compound. The concentration of solvents used in the experiment was always below 0.05%. The

concentrations of the inhibitors used in the experiments were determined as in previous studies by Badger et. al., 1999 (15). Cell viability, morphology and monolayer confluency were assed to rule out cytotoxic effects of the inhibitor. Results were exhibited as a function of efficiency and ability of InhA in degrading TJ protein ZO-1 with and without inhibitors in western blot and immunofluorescence analysis (116).

HBMEC infection, invasion and antibody protection assays

Cells were grown to confluence in collagen-coated 24 well culture plates. Cell monolayers were washed three times with HBSS and reconstituted in XM containing bacterial a multiplicity of infection of 1:10. All culture plates were centrifuged at 800 x g for approximately 5 min to ensure synchronization of infection. Immediately after centrifugation, cells were placed in an incubator for 4 hours at 37 º C with 5% CO_2. To remove excess extracellular bacteria HBMEC were washed 3 times with Hank's balanced salt solution (HBSS) before adding a mixture of XM plus 50 µg/ml of gentamicin for 30 min. Prior control experiments (data not shown) showed that both *B. anthracis and B.subtilis* were killed with 50 µg/ml of gentamicin within 30 min of exposure. To ensure the removal of gentamicin (Catalog No. G1397; Sigma), cells were washed 3 times with HBSS prior to adding 0.1 ml of 0.25% trypsin/EDTA solution (5 min 37ºC) following the addition of 0.4 ml of 0.025% Triton X-100 to extract intracellular bacteria. The amount of intracellular bacteria was quantified by different dilutions of HBMEC lysate on LB agar plates. Transformed InhA expressing *B. substilis* spores were provided as a kind gift from Nalini Ramarao at the Institut National de la Recherche Agronomique (Paris, France) and wild-type *B. substilis* was obtained from ATCC (Manassas, VA).

For the antibody protection assay, *B. anthracis* spore cultures were treated with different concentrations of InhA-specific and Iso-type control antibodies for 30 min before its addition to HBMEC monolayer. The quantification of intracellular bacteria was determined as previously described (121). All assays were repeated at least 3 times and triplicates were done of each condition.

Protein extraction, SDS-PAGE and western blot analysis

HBMEC monolayers were washed twice with HBSS before adding 1x RIPA buffer (Catalog No. 89900; Pierce, Rockford, IL) containing 1% Triton X-100 (Sigma) and 1x protease inhibitor cocktail (Catalog No. 89806; Pierce, Rockford, IL) to extract cell lysate. Cell lysates were further broken down using 24 gauge needle and 1 ml syringe. Samples were centrifuged at 14,000 x g for 10 min and supernatant collected and boiled in SDS sample buffer containing 30 mM dithiothreitol (DTT, Catalog No. D9779; Sigma). Proteins were loaded on to 4-12% and 6% Bis-Tris and Tris-Glycine Gel (Invitrogen). Proteins were transferred to nitrocellulose membrane using the iBlot Gel Transfer System (Invitrogen). The membranes were blocked with 5% milk powder in PBS solution and probed with antibodies against ZO-1(Catalog No. 40-2300; Invitrogen), occludin (Catalog No. 40-6100; Invitrogen), claudin-1 (Catalog No. 37-4900; Invitrogen) and JAM-1 (Catalog No. 04-593; Chemicon). After washings, blots were incubated with appropriate peroxidase-coupled secondary antibodies (Amersham Biosciences, Piscataway, NJ) and developed with Super Signal West- Femto Chemiluminescent Substrate (Catalog No. 34080; Pierce, Rockford, IL). Visualization of blots was done on ChemiDoc XRS (BioRad, Hercules, CA).

Immunostaining and fluorescence microscopy

HBMEC were seeded on Biocoats 8-well Culture slides from BD falcon at 20,000 cells per well. The cells were incubated for approximately 3 days. After treatment, at the designated time point, cells were washed three times with PBS and fixed with 2% paraformaldehyde in PBS for 15 min at room temperature and permeabilized with 0.5% Triton X-100 in PBS for 20 min. The monolayers were first incubated with mouse anti-human ZO-1and rabbit anti-human InhA antibody (Catalog No. 40-2300; Invitrogen), or goat anti-mouse ZO-1 in PBS containing 5% fetal calf serum (FCS; Sigma) for 1 hour, washed three times with PBS, and then incubated with FITC-conjugated donkey anti-goat and donkey anti-rabbit antibodies in PBS containing 5% FCS. Cells were washed with PBS, chambers were removed, and slides were mounted with DAPI ProLong Gold Antifade Reagent (Catalog No. P36931; Invitrogen) and coversliped. Stained cells were visualized with a Nikon confocal microscope.

Tissue section slides were deparaffinized and re-hydrated. Slides were washed and fixed with 4% paraformaldehyde for 10 min. Sections were rinsed three times with PBS and blocked with 1.5% goat serum solution (in PBS) for 30 min at 4ºC. Slides were washed again and primary antibody for anti-InhA was incubated in humid chamber at 4ºC overnight. Slides were washed, incubated with appropriate secondary antibody and mounted according to above mentioned protocol. Visualization of InhA and quantum dots nanoparticles were done using fluorescence microscope (Nikon). The custom-made InhA antibody from Zymed/Invitrogen was developed against the N-terminal region of the active form of the metalloprotease InhA. Rabbits were injected with the peptide for the

N-terminal region (sequence: CPAKQKAYNGDVRKD-amide) of InhA (BA1295 of *B. anthracis*). Rabbits were exsanguinated, and peptide affinity purification was performed to purify antibody from serum.

For co-localization of InhA with ZO-1, purified InhA was conjugated to FITC flurophore using the EZ-Label FITC Labeling Kit (Catalog No. 53004; Pierce, Rockford, IL). The conjugation of the flurophore were carried out according to procedures provide in the kits. In short, purified InhA was dialyzed and exchanged into borate buffer. Optimal molar ratios of FITC to InhA was deduced. InhA, FITC, and DMF (Dimethylformamide) were combined in the FITC labeling reaction. Excess unbound FITC was removed by dialysis. For the controls, labeling procedure for FITC was repeated but without purified protein present. HBMEC were treated with FITC-conjugated InhA and FITC alone, washed several times after designated time points. Immunofluorescence of ZO-1 and InhA was conducted according to the previously mentioned protocol above.

For localization InhA in mouse brain, purified InhA was conjugated to nanoparticles using the Qdot® ITK™ Carboxyl Quantum Dots to Steptavidin protocol from Invitrogen. Enzymatically active InhA, nanoparticles, and EDC (1-ethyl-3-(3-dimethylaminopropyl) carbodiimide hydrochloride) were combined in the labeling reaction. Excess unbound InhA was removed from the nanoparticles by syringe filtration and centrifugation using ultrafiltration unit (100 kDa cutoff). For the controls, labeling procedures for nanoparticles were repeated, but without purified protein present or with

heat-inactivated purified protein (InhA) present. Immunofluorescence of nanoparticles and InhA were visualized according to the previously mentioned protocol above.

Cytokine array

The levels of cytokines released into culture media induced by InhA were measured using RayBio Human Cytokine Antibody Array 3 (Catalog No. AAH-CYT-3; RayBiotech, Norcross, GA)**.** The array provides a qualitative Western screening technique. The standard array matrix consisted of a dot grid on a nitrocellulose membrane with a total of 42 capture antibodies. Array kit included an instruction manual and with the biotinylated-antibodies solution. 24 h culture medium from control and InhA treated HBMEC cell medium was collected. 1 ml of this medium was added to the cytokine array membrane and incubated for 2 h. The membrane was washed three times with washing buffer I for 5 min each, and then with washing buffer II for 5min each. Cytokine was detected using cytokine antibodies for 1 h, followed by HRP-labeled strepavidin incubation for 1 h. All dilutions used for each of these reagents were suggested by the instructions contained in the assay kit. The membranes were developed by Super Signal West Femto Chemiluminescent Substrate (Pierce, Rockford, IL) and visualized with ChemiDoc XRS (BioRad, Hercules, CA).

ZO-1 digestion in Naïve HBMEC lysate and purified rZO-1 by InhA

Naïve cell lysates from HBMEC and rZO-1 protein were treated with different concentrations of InhA (1, 0.1, and 0.01 μg/ml) and incubated at 37º C for 4 h. SDS-PAGE and Western blot were done using anti-ZO-1 antibodies (for lysate) (Catalog No.

40-2300, Invitrogen) or α-His antibodies (for rZO-1, Invitrogen). Cleavage domains of the ZO-1 protein after incubation of InhA were estimated by His-antibody-western blot mapping.

Construction of recombinant ZO-1 protein fragment

N-terminal primer (5'-ATG CTG AGA TGA AGG TAT CAG-3') and a C-terminal primer (5'-TCA GAT GTA GGA GAT TCT TTC-3') were ordered from and synthesized at Invitrogen. The primers were made according to appropriate melting temp and base pair length. Homo sapien TJ protein cDNA clone was ordered from ATCC (Manassas, VA), Gene Bank Number: BC111712. Colonies of the clone were selected from the tilt culture tube and grown. PCR was done using the above described primers. A total of 30 cycles were done. A cycle profile was chosen to best fit the primers and the template DNA at hand (94ºC-5 min; 94 ºC-30 sec; 55 ºC – 30 sec; 72 ºC – 5 min; 72 ºC – 10 min and 4 ºC cool down). Protocol for Platinum Blue PCR Supermix 96 was used (Catalog No. 12580; Invitrogen). The PCR product was purified by using a PCR purification kit (Qiagen) and cloned into plasmid pTRcHis II TOPO plasmid (Invitrogen) encoding ampicillin and kanamycin resistance by using the TOPO TA cloning kit (Catalog No. K4410-01; Invitrogen) according to the instructions provided. pTRcHis II TOPO transformed into DH5-alpha *E. coli* cells. The culture was then plated on ampicilin LB agar plates overnight to select for positive transformants. Verification of transformant with appropriate orientation of ZO-1 DNA was done using restriction enzymes. Correct orientation transformants were selected and grown. Recombinant ZO-1 proteins were prepared by IPTG (Invitrogen) induction and purified by ProBond™

Nickel-Chelating Resin (Catalog No. R801; Invitrogen). The proteins samples were run confirmed by Western blot with anti-ZO-1 antibodies (Invitrogen). Visualization was done as stated in the section above.

In vivo BBB permeability assays

Female, 9-week old DBA/2 mice were purchased from Jackson Laboratory (Bar Harbor, ME). Mice were maintained at Biocon, Inc. (Rockville, MD). The George Mason University Institutional Animal Care and Use Committee and the Biocon, Inc. Animal Care and Use Committee/Institutional Review Board have approved all protocols prior to animal experiments. Mice were anesthetized and then injected intravenously via the intra-orbital route with InhA (1 U per mouse). Control animals were injected PBS with the same volume of InhA. Approximately 1 hour before each time point, animals were injected with a 100 µl of Evans blue (EB, Catalog No. E2129; Sigma) dye (1% w/v solution) through the tail vein and then perfused with 10 ml of PBS 1 h later through the apex of the heart. The brains were then removed, weighed, homogenized in 1.5 ml of PBS. To extract the EB dye from the tissue homogenate, 1.5 ml of trichloroacetic acid (60% w/v) was added to each sample. The homogenate solution was vortexed for 2 min and then centrifuged for 30 min at 4 º C at 1000 x g. The EB supernatant was collected and analyzed on colorimetric plate reader at 620 nm and the background subtracted. The background (base-line absorbance) will be calculated by measuring absorbance at 620 nm and divided by the wet weight of the whole brain (122; 123). Standard was done of EB dye to extrapolate the amount of EB in each sample. EB data was expressed as µg EB dye/g of brain.

For histopathological and immunofluorescence studies, mice were anesthetized to prevent any discomfort or injury. Mice were injected intravenously via the intra-orbital sinus with 1U in 100 µl of active protease and inactive protease labeled with Quantum Dot Nanoparticles (Catalog No. Q2130MF; Invitrogen). Control mice were injected with quantum dots nanoparticles alone (same volume). After approximately 24 h, mice were deeply anesthetized and then euthanized using cervical dislocation. The brains removed and immersed in the fixative (10% buffed formalin). Samples brains were sectioned by AML Laboratories (Rosedale, MD). Paraffin-imbedded samples (5 µm) were stained with hematoxylin and eosin. For the immunofluorescence staining, sections were prepared as stated above.

4. RESULTS

Induction of Barrier Permeability by B.anthracis in HBMEC and ARPE-19 Cells

To examine the possible effect of the *B. anthracis* on human BBB (HBMEC monolayer) and human retinal pigment epithelial (ARPE-19 cells) BRB integrity in their *in vitro* models, a real-time transendothelial / transepithelial electrical resistance (TEER) was measured. These measures quantify barrier integrity, which represents changes in the permeability of the monolayers. As shown in Figures 7 and 8, both Sterne and Δ Sterne of *B. anthracis*-treated HBMEC and ARPE-19 cells had progressive drop in TEER with time. At 24 h, TEER of both cell lines had dropped to base line 400 Ω, indicating permanent loss in monolayer resistance. Cell monolayer (ARPE-19 cells and HBMEC) were treated with a ratio of 1:10 multiplicity of infection of cells to spores. No significant difference in TEER drop between the toxigenic (Sterne) and non-toxigenic (Δ Sterne) strains was observed in either of HBMEC and ARPE-19 cells. However, ARPE-19 cells were somewhat resistant to bacteria-induced TEER drop than HBMEC.

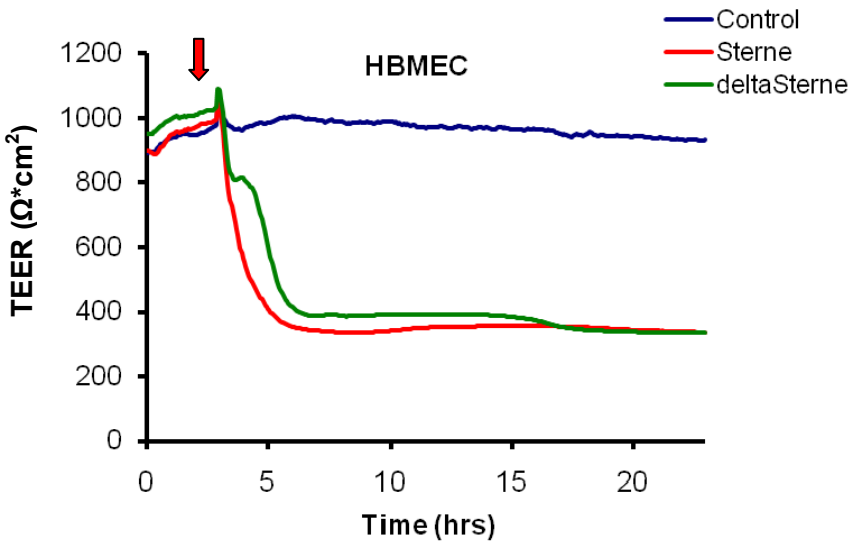

Figure 7. Real-time trans-endothelial electrical resistance (TEER) of bacteria-challenged HBMEC monolayer.
HBMEC were challenged with 1:10 MOI of *B. anthracis* Sterne (red) and Δ-Sterne (green) and incubated at 37º C for 24 h. Both the toxigenic and non-toxigenic bacteria strains caused a marked decrease in TEER in HBMEC monolayer compared to untreated control (blue). The arrow marks the addition of bacteria. Experiments were done in tandem and TEER measurements are an average of 2 wells. Measurements were automatically obtained in two min intervals for a 24 h period.

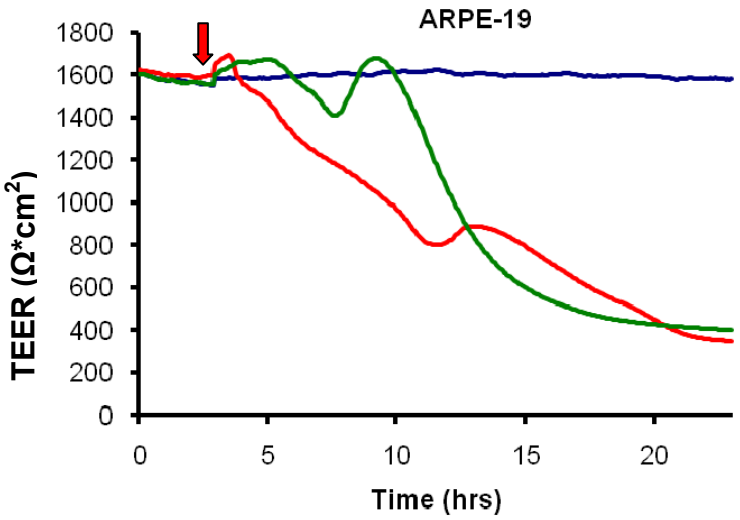

Figure 8. Real-time trans-endothelial electrical resistance (TEER) of bacteria-challenged ARPE-19 cell monolayer.
ARPE-19 cells were challenged with 1:10 MOI of *B. anthracis* Sterne (red) and Δ-Sterne (green) and incubated at 37º C for 24 h. Both the toxigenic and non-toxigenic bacteria strains caused a marked decrease in TEER in HBMEC monolayer compared to untreated control (blue). The arrow marks the addition of bacteria. Experiments were done in tandem and TEER measurements are an average of 2 wells. Measurements were automatically obtained in two min intervals for a 24 h period.

Induction of barrier permeability in HBMEC by secreted anthrax protease InhA

The potential effect of the anthrax metalloprotease InhA on human BBB (HBMEC monolayer) and human retinal pigment epithelial BRB integrity was examined *in vitro*. A real-time transendothelial electrical resistance (TEER) was used to measure the barrier integrity, which represents changes in the permeability of the monolayer. As shown in Figure 9A, InhA-treated HBMEC had progressive drop in TEER with time, unlike ARPE-19 cell where no decrease in TEER was recorded as seen in Figure 10A. At 24 h, TEER of HBMEC had dropped approximately 60 percent relative to control,

indicating permanent loss in monolayer resistance. In contrast, control untreated HBMEC and ARPE-19 cells did not have a decrease in TEER; rather, monolayer resistance showed a slight but non-significant increased as a function of time. Cells treated (ARPE-19 cells and HBMEC) with 1 μg/ml of Npr599 did not show a decrease in TEER. A slight increased was recorded. Phase contrast microscopy was performed on HBMEC (Figure 9B) and ARPE-19 cells (Figure 10B) monolayer after 24 h treatment with InhA (1 μg/ml) and Npr599 (1 μg/ml) in ECIS 8-well culture slides at 37ºC. Using differential interference contrast microscopy (DIC), pictures of the monolayers were taken at 24 h to further assess its integrity (Figure 10B). HBMEC treated with InhA showed gaps in the monolayer with detachment and disappearance of cells from the slide surface. In the untreated HBMEC, InhA-treated/untreated APRE-19 cells and Npr599-treated cells, the monolayer was intact with no obvious dysmorphology. Together, these results suggest that InhA is capable of inducing barrier permeability in HBMEC and not ARPE-19 cells.

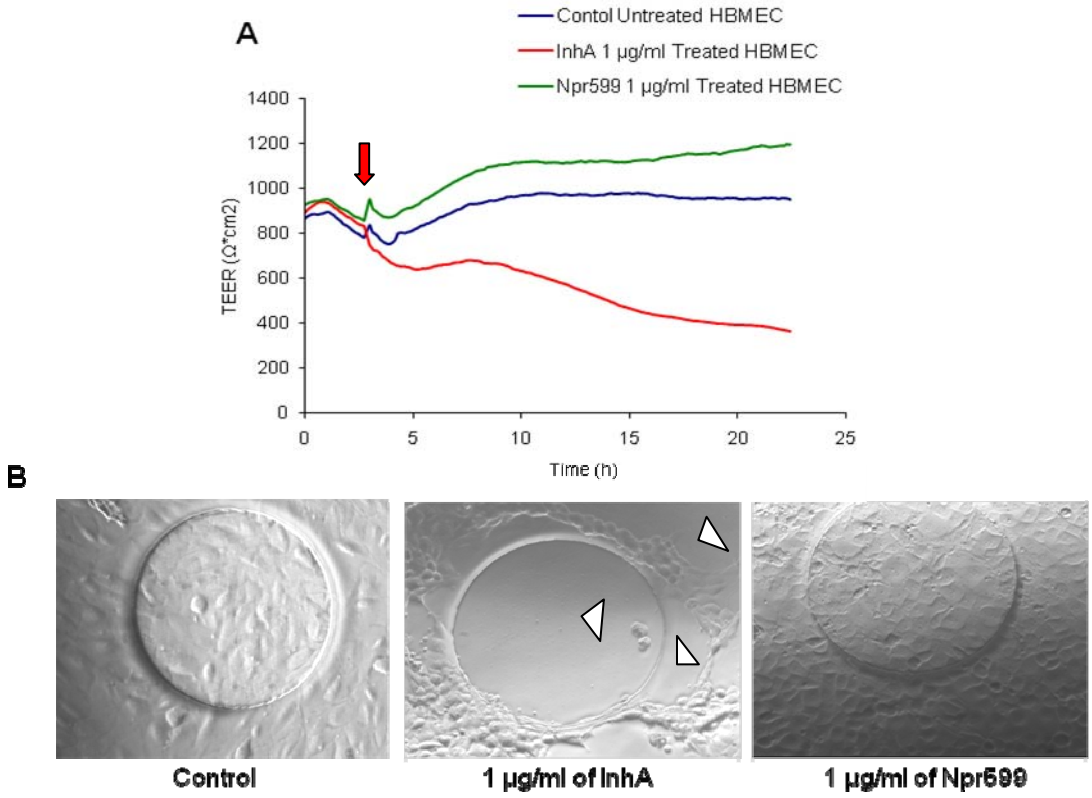

Figure 9. Real-time trans-endothelial electrical resistance (TEER) of HBMEC monolayer and phase contrast microscopy.
(A) HBMEC were treated with 1 µg/ml InhA (red) and incubated at 37º C for 24 h. InhA caused a marked decrease in TEER in HBMEC monolayer compared to untreated control (blue) and 1 µg/ml Npr599 treated-HBMEC (green). The arrow marks the addition of protease. (B) Phase contrast microscopy of HBMEC monolayer was taken immediately after 24 h time point. The arrowheads point to gaps formed in the monolayer of HBMEC after treatment with 1µg/ml of InhA (center); 1 µg/ml of Npr599-treated HBMEC (right) and the untreated control (left). Pictures were taken at 100x magnification. Experiments were done in tandem and TEER measurements are an average of 2 wells. Measurements were automatically obtained in two min intervals for a 24 h period.

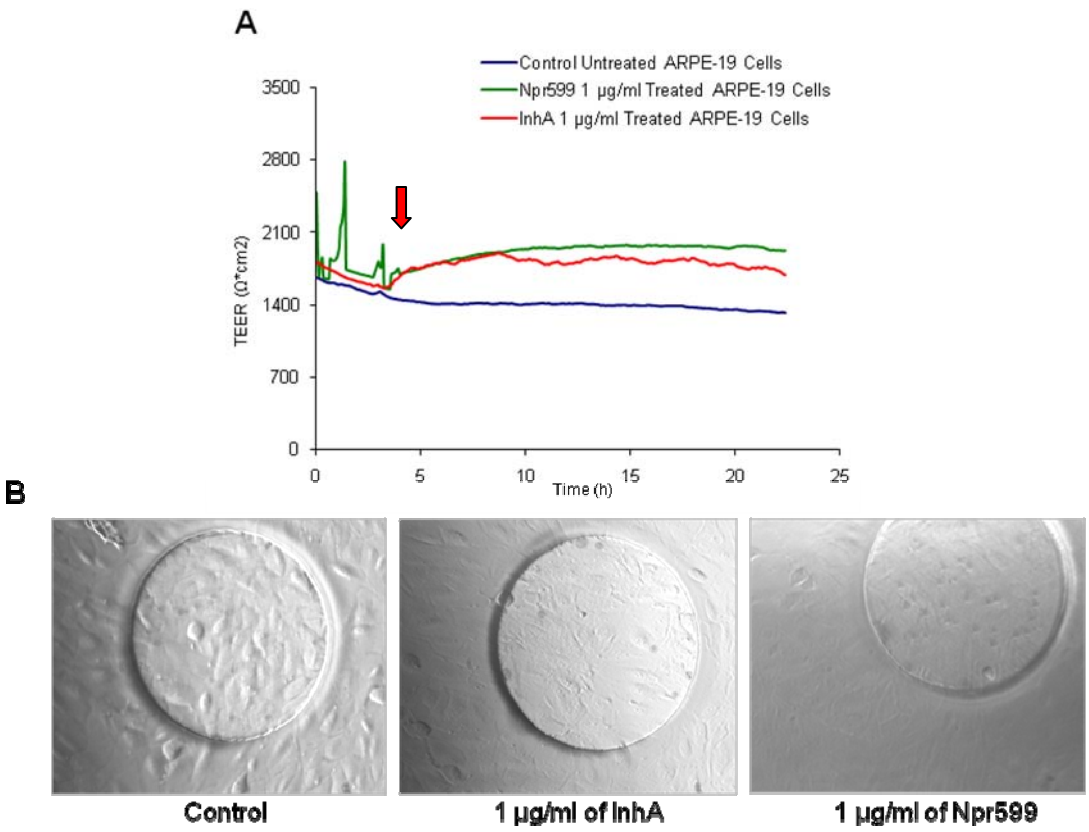

Figure 10. Real-time trans-epithelial electrical resistance (TEER) of ARPE-19 monolayer and phase contrast microscopy.
(A) ARPE-19 were treated with 1 µg/ml InhA (red) and 1 µg/ml Npr599 treated-HBMEC (green), incubated at 37º C for 24 h. Neither InhA nor Npr599 caused a marked decrease in TEER in ARPE-19 cell monolayer compared to untreated control (blue). The arrow marks the addition of protease. (B) Phase contrast microscopy of ARPE-19 cell monolayer was taken immediately after 24 h time point. Pictures after treatment with 1µg/ml of InhA (center); 1 µg/ml of Npr599-treated ARPE-19 cells (right), and the untreated control (left). Pictures were taken at 100x magnification. Experiments were done in tandem and TEER measurements are an average of 2 wells. Measurements were automatically obtained in two min intervals for a 24 h period.

Effect of InhA enzymatic activity on TJ components of HBMEC

BBB function is defined by the state of its TJ proteins and associated proteins. Studies have indicated that a decrease in barrier function is directly correlated to loss of junctional proteins (46). It was therefore imperative to examine whether the enzymatic activity of InhA or the protein itself can cause degradation of tight junction proteins in HBMEC. Western blot analysis showed that the active form of InhA at 1 μg/ml is capable of degrading ZO-1 but not claudin-1, occludin, and JAM-1 after 24 h, indicating that only ZO-1 may be a target of InhA in HBMEC (Figure 11A). The densitometric analysis of InhA-induced ZO-1 degradation is illustrated in Figure 11B. Concentration-dependent proteolysis of ZO-1 was observed in InhA-treated HBMEC; drastic and significant decline in ZO-1 levels occurred with increasing concentrations of 1 μg/ml to 3 μg/ml of InhA. Moreover, heat-inactivated InhA did not degrade any of the above mentioned tight-junction proteins (data not shown). This indicates that InhA enzymatic activity is involved in the process of degradation of ZO-1 protein.

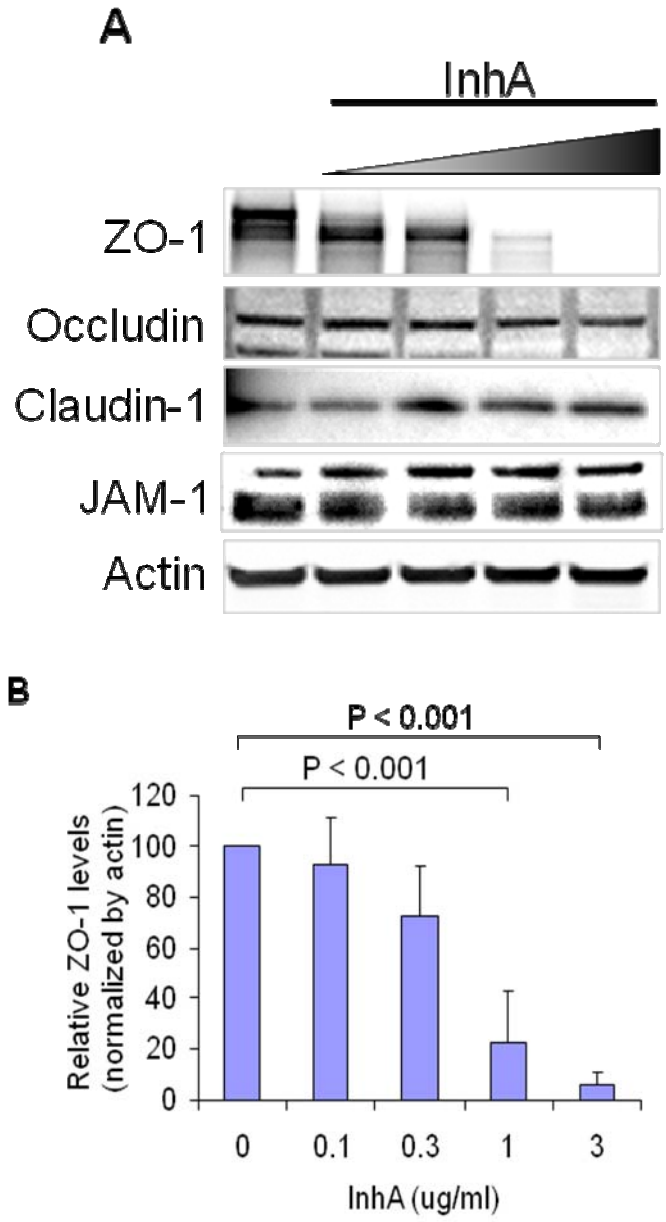

Figure 11. Western blot of tight-junction proteins in HBMEC after treatment with InhA and desitometric analysis of ZO-1 protein.
(A) HBMEC cells were treated with increasing concentrations of InhA (0.1, 0.3, 1, 3 μg/ml from left to right) for 24 hr at 37º C. Western blots were probed with antibodies to ZO-1 (225 kDa), occludin (56 kDa), claudin-1(22 kDa), and JAM-1 (39 kDa). A represented immunoblot is shown for the tight- junctional proteins from 4 experiments. β-actin was used as a control. (B) Densitometry was conducted to quantify loss in the amount of ZO-1 protein in the western blot analysis. All samples analyzed were normalized to β-actin. Data are mean ± SD (n=4).

InhA is able to directly degrade and cleave ZO-1 protein

ZO-1 functions as a key component in the BBB and associates with several different integral membrane and cytosolic proteins of the TJs; these include occludin, claudins, JAMs, and AF6 (124-126). Given that ZO-1 has multivalent associations and is important in the BBB function, we continued to study its proteolytic nature and target. It was necessary to examine whether the observed proteolytic action on ZO-1 in HBMEC presented above can be attributed to InhA alone, or to other cellular proteases that might be activated. We incubated naive HBMEC cell lysate with different concentrations of InhA to verify its direct proteolytic activity. As shown in the western blot analysis, a dose-dependent cleavage of ZO-1 occurs producing several fragments (Figure 12). Further, to rule out other factors acting upon the cell and to validate these results (Figure 13), purified recombinant domain of ZO-1 (rZO-1) was incubated with InhA over different time points. The western blot in Figure 13A shows several fragments of rZO-1 of 34.6, 36.8, 38.9, 44.8, and 55.5 kDa after incubation with InhA at 37ºC. Time-dependent degradation of rZO-1 was observed as early as 1 min, with total disappearance of the recombinant fragments by 10 min. These experiments suggest that ZO-1 is directly cleaved by InhA. The cleavage sites were shown to be concentrated in the regions between MAGUK and α-domains. We were able to create a model of the putative cleavage sites based on the molecular weight of the fragments seen in the His-tag Western blot (Figure 13B, lower panel).

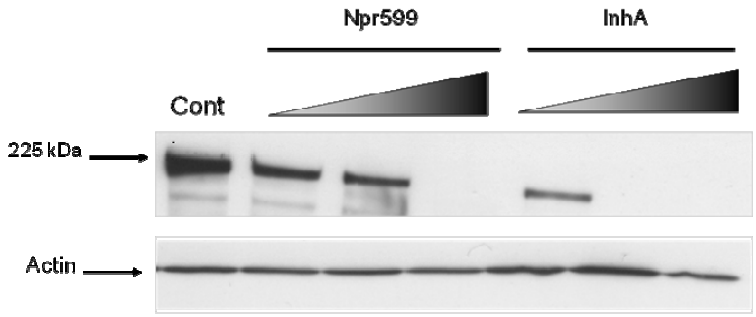

Figure 12. Concentration-dependent and time-dependent cleavage ZO-1 in naïve cell lysate.
Western blot shows a concentration-dependent cleavage of ZO-1 in naïve HBMEC lysate by added InhA and Npr599 (at 0.001, 0.01, 0.1 µg/ml left to right), incubated at 37º C for 4 h. Cont = untreated cells.

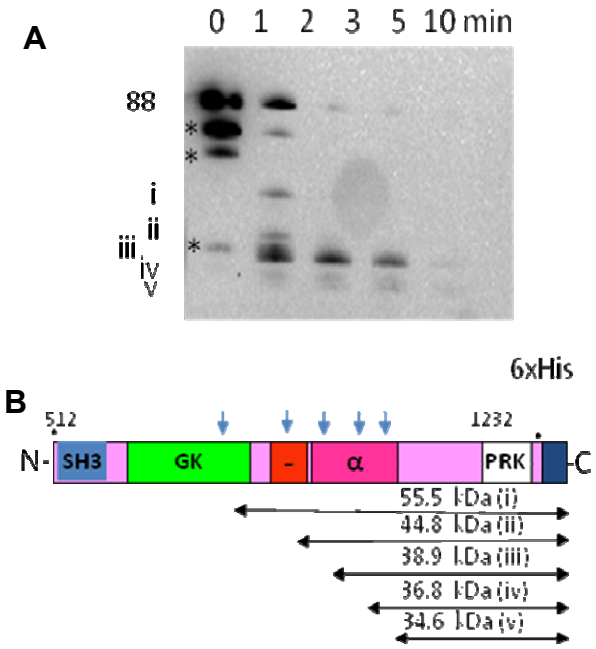

Figure 13. (A) Western blot of histidine-tagged rZO-1 with anti-his antibodies. Degradation of purified rZO-1 after treatment with 0.1 µg/ml InhA for 1 min, 2 min, 3 min, 5 min, and 10 min at 37º C. (B) Putative cleavage sites of middle segment rZO-1 (roman numerals /blue arrows) after treatment with InhA were deduced by molecular weight from immunoblot. Asterisks represent non-specific cleavage of recombinant protein due to purification. The cleavage sites were shown to be concentrated in the region between MAGUK and alpha domains of ZO-1.

Time-dependent effects of InhA on ZO-1 in HBMEC

To characterize InhA's enzymatic action on ZO-1 within cells, a time-dependent study was conducted for determining how quickly InhA could degrade ZO-1 in HBMEC. Cells were incubated with 1 μg/ml of InhA at different time points. Western blots were probed with anti-ZO-1 antibodies (Figure 14). Degradation of ZO-1 in HBMEC can be observed as early as 20 min, with complete loss of protein observed at 20 h. Notably however, Npr599 was unable to cleave ZO-1 in HBMEC.

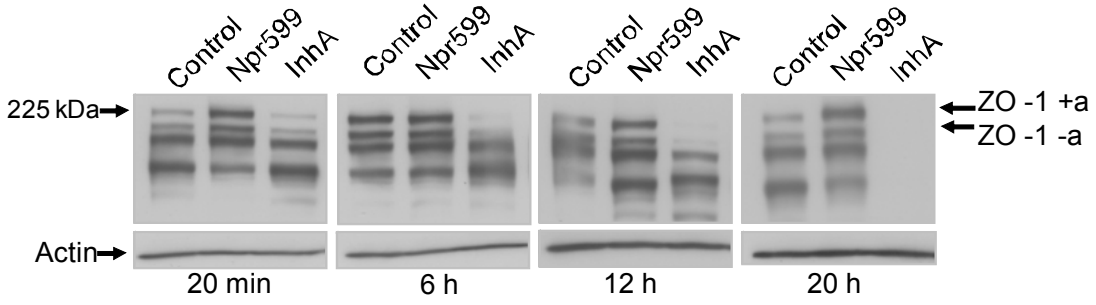

Figure 14. Western blot analysis of time-dependent degradation of ZO-1 in HBMEC (20 min, 6 h, 12 h, 16 h, 20 h). Actin was used a loading control. The black arrows indicate the two isoforms for ZO-1. Lower bands in blot are non-specific or represent products of degradation of original 125 kDa band. A represented immunoblot was shown for all western blots, each observation was repeated 4 times.

Evidence for endocytosis of InhA, using specific eukaryotic cytoskeletal inhibitors

We investigated the potential involvement of endocytic processes in InhA's action on ZO-1, using specific eukaryotic cytoskeletal inhibitors. To identify the integral role of cellular cytoskeleton in InhA-induced degradation of ZO-1 in HBMEC, we studied the effect of cytochalasin D, an actin polymerization inhibitor (127). Confluent HBMEC were incubated with cytochalasin D prior to InhA treatment at varying concentrations.

Lysate samples were collected and Western blot analysis was performed using antibodies to ZO-1. Cytochalasin D at 0.25 μg/ml prevented InhA-induced (0.1 μg/ml) degradation of ZO-1 in HBMEC (Figure 15). In addition to our Western data, we also conducted experiments to monitor ZO-1 integrity by immunofluorescence microscopy.

In the absence of the inhibitor, loss of ZO-1 was clearly observed in cells treated with InhA (0.3 μg/ml) alone. In contrast, cells pre-treated with cytochalasin D did not show any degradation of ZO-1 after treatment with InhA (Figure 16d). Cells treated with cytochalasin D alone did not show any effect (Figure 16c). The concentrations used in these experiments were determined in accordance with the previous study of Badger et al., 1999 (117). Consistent with their results, we did not observe any morphological changes in HBMEC treated at 0.25 μg/ml.

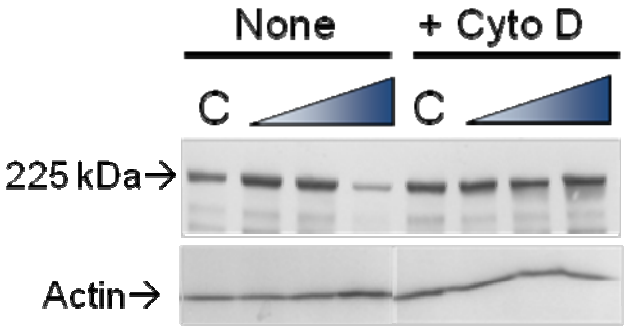

Figure 15. Protective effect of eukaryotic cytoactive agent cytochalasin D on InhA-induced degradation of ZO-1 in HBMEC and colocalization of InhA with ZO-1.
Western blot analysis of ZO-1 from HBMEC treated with or without 0.25 μg/ml of cytochalasin D for 1 h prior to incubation with varying concentrations of InhA (0.001, 0.01, 0.1 μg/ml) at 37° C for 12 h. Triangles represent increasing concentration of InhA.

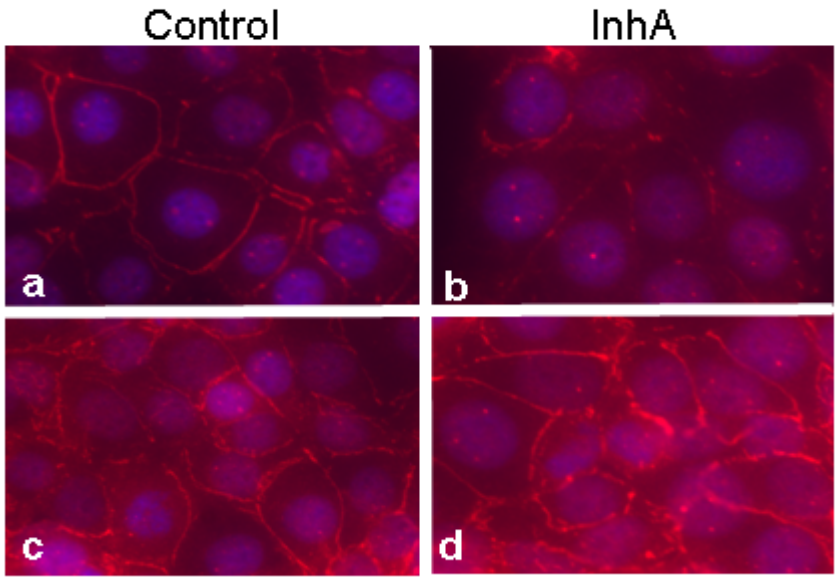

Figure 16. Protective effect of eukaryotic cytoactive agents (cytochalasin D) on InhA-induced degradation of ZO-1 in HBMEC and colocalization of InhA with ZO-1.
Immunofluorescence of ZO-1 in HBMEC. (a) untreated HBMEC. (b) InhA-treated HBMEC. (c) Cytochalasin D-treated HBMEC. (d) Cytochalasin D→InhA-treated HBMEC. ZO-1 (red) and DAPI (blue).

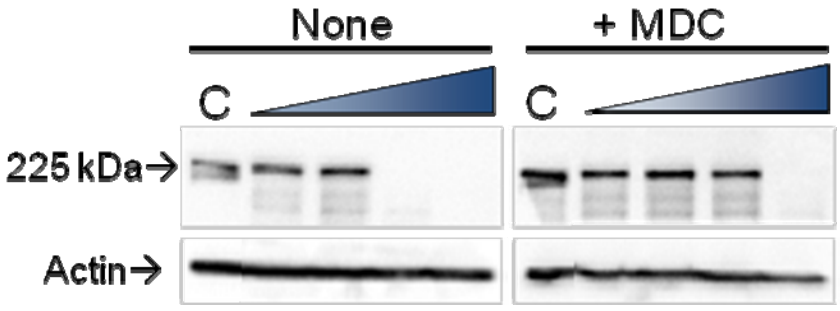

Figure 17. Protective effect of eukaryotic cytoactive agents MDC on InhA-induced degradation of ZO-1 in HBMEC.
Western blot analysis of ZO-1 from HBMEC treated with or without 2.5 µg/ml of monodansylcadaverine (MDC) for 30 min prior to incubation with different concentration of InhA (0.001, 0.01, 1, 3 µg/ml) at 37º C for 12 h.

Inhibition of clathrin-coated pit formation, clustering, and internalization of the ligand-receptor complexes have been shown to be mediated by monodansylcadaverine (MDC) (128; 129). InhA was added in different concentrations to HBMEC treated with and without MDC. Western blot analysis probed with anti-ZO-1 antibodies showed, MDC at 2.5 μg/ml per well prevented InhA-mediated degradation of ZO-1 in HBMEC, and was able to protect ZO-1 from being degraded at concentrations of up to 3 μg/ml InhA (Figure 17). The concentrations of MDC in this experiment were well below the suggested cytotoxicity level as observed by Badger et al., 1999 (117). These results suggest that InhA-induced degradation of ZO-1 of HBMEC is partially dependent on eukaryotic processes of clathrin-coated pit formation and microfilament polymerization, which are characteristic of the endocytotic process.

InhA is able to co-localize with ZO-1 of HBMEC.

Our observations that ZO-1 proteolysis by InhA may involve eukaryotic cytoskeletal components prompted us to study co-localization InhA and ZO-1 (Figure 18). The localization of InhA was observed using immunofluorescence microscopy. HBMEC were treated with either FITC fluorophore alone or with 10 μg/ml of InhA labeled with FITC fluorophores. Following the addition of FITC-labeled InhA to HBMEC for 1 min incubation, possible co-localization of InhA-FITC (e.g., green signal) with ZO-1 (e.g., red signal) was observed in the periphery of HBMEC cells, suggesting its localized aggregation (i.e., yellow signal), along with peripheral degradation (center frame). After 2 min of incubation, InhA appeared to be partially co-localized with ZO-1 in the cytoplasm of the cell and surrounding the nucleus. Additionally, experiments in

which cells were immunostained for ZO-1 and FITC fluorophore alone (control monolayer for both 1 and 2 min time points; left frame) presented no visual evidence of FITC fluorescence. This provides further insight as to the mechanism involved in InhA uptake into HBMEC. These data illustrate that InhA tends to be associated with with ZO-1 of HBMEC, which suggests the possibility of their co-localization.

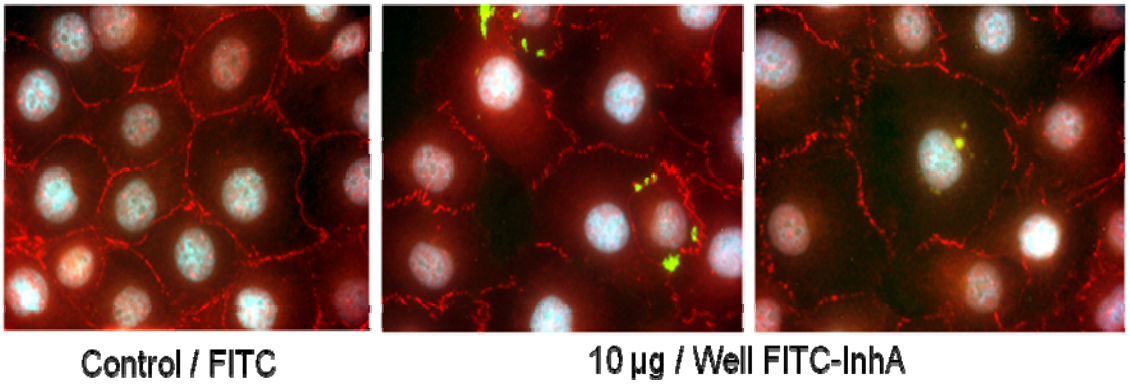

Figure 18. Possible co-localization of FITC-labeled InhA with ZO-1 in HBMEC. Cells were treated with FITC-conjugated InhA (10 µg/ml) and FITC alone for 1 min and 2 min. Cells were washed 5 times before fixation. Immunofluorescence microscopy for ZO-1 was conducted. A loss of ZO-1 was observed in both time points. At 1 min FITC-conjugated InhA was colocalized around ZO-1. After 2 min, FITC-conjugated InhA colocalized to cell nucleus.

InhA protein is implicated in the invasion of HBMEC

Our studies employing eukaryotic cell inhibitors *e.g.*, cytochalasin D suggested that the endocytosis of InhA can potentially take place in HBMEC. It has also been shown that InhA may play a role in macrophage membrane permeability (130). Moreover, InhA protein is not only secreted, but also found, to be a major component on

the *Bacillus* species exosporium (131; 130). We took non-pathogenic spores of *B. subtilis* InhA-deficient wild-type and spores of *Bacillus subtilis* transformed with InhA mutants and tested their efficiency invasion into HBMEC. The invasion assays were performed showing approximately a 24-fold increase in intracellular *B. subtilis* transformed InhA mutants compared to the wild-type InhA-deficient *B. subtilis* (Figure 19). To further define the role of InhA in HBMEC invasion, we conducted an antibody protection assay using antibodies specific to InhA. *B. anthracis* spores were pre-incubated (30 min) with 20 μg/ml of InhA antibodies and isotype IgG control, and added to HBMEC monolayer. The number of intracellular bacteria at 4 h was decreased more than 3-fold decrease in the *B. anthracis* InhA transformed mutant treated with anti-InhA antibodies compared to *B. anthracis* InhA transformed mutants treated with iso-type control IgGs (Figure 20). These experiments provide additional functional evidence for InhA's access to ZO-1 in HBMEC through an endocytic process.

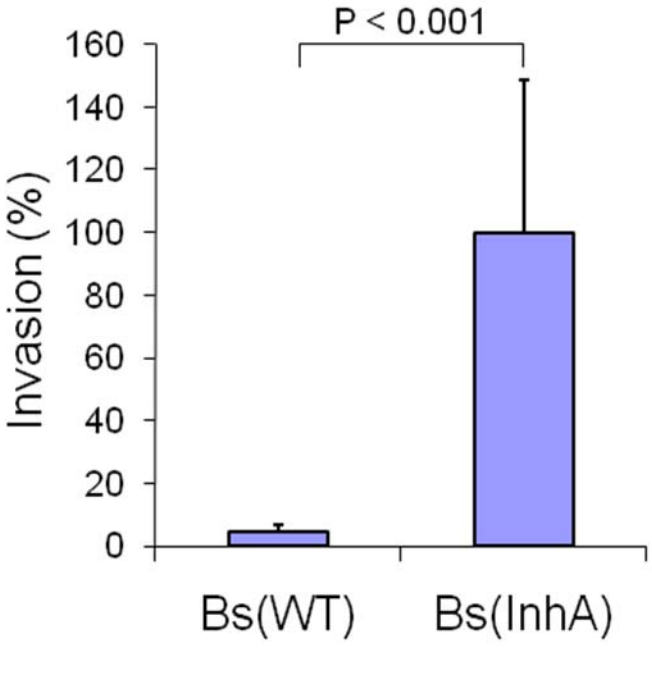

Figure 19. Invasion of wild-type spores vs. mutant spore into HBMEC.
Invasion of wild-type *B. subtilis* (InhA-deficient) spores (Bs(WT)) and spores of *B. subtilis* transformed InhA-mutants (Bs (InhA)) ($p < 0.001$) into HBMEC. Data were initially collected in intracellular colony forming units (CFU) with an MOI 1:10. Data are represented in percent relative to control. All data were repeated at least three times with samples triplicates done in each condition.

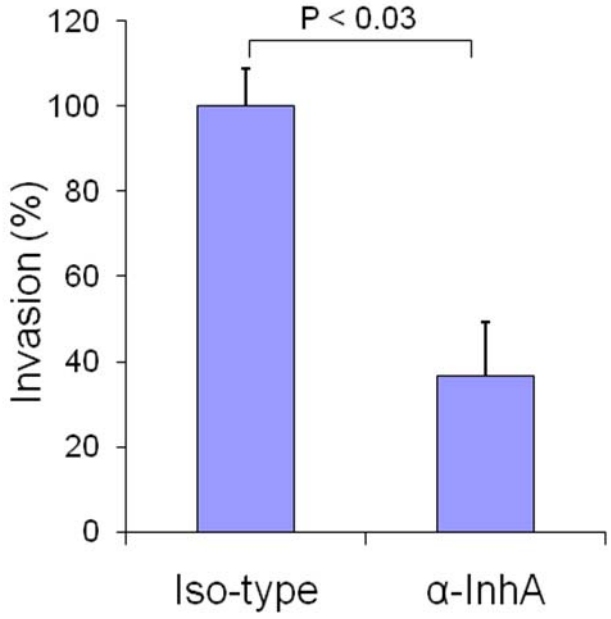

Figure 20. InhA-antibody inhibition assay.
Inhibition of *B. anthracis* HBMEC invasion by rabbit InhA-specific antibodies (20 μG/ml)s compared to isotype (rabbit IgG) control ($p < 0.03$) Data were initially collected in intracellular colony forming units (CFU) with an MOI 1:10. Data are represented in percent relative to control. All data were repeated at least three times with samples triplicates done in each condition.

Cytokine profile of InhA- treated and -untreated HBMEC.

We considered that host cytokine release during infection might have some effects on the barrier integrity. To assess that possibility a membrane-bound antibody array technique was employed to characterize the release of cytokines in the InhA-treated and untreated HBMEC-conditioned media. A map of the array membrane is displayed in Figure 21C. The media from a 24 h culture of both untreated and InhA-treated HBMEC produced immune-positive signals in cytokines for Gro, Gro-α, IL-6, IL-8 and MCP-1

(Figure 21A and 21B). The main difference was, slightly higher intensity was observed in InhA-treated HBMEC culture media for monocyte chemotactant protein-1 (MCP-1) (Figure 21B). Six identical positive control and three negative control antibodies were observed in both untreated and InhA-treated HBMEC cultured media. From these data it appears that in our experimental condition cytokines may not play an important role in InhA-induced BBB disruption.

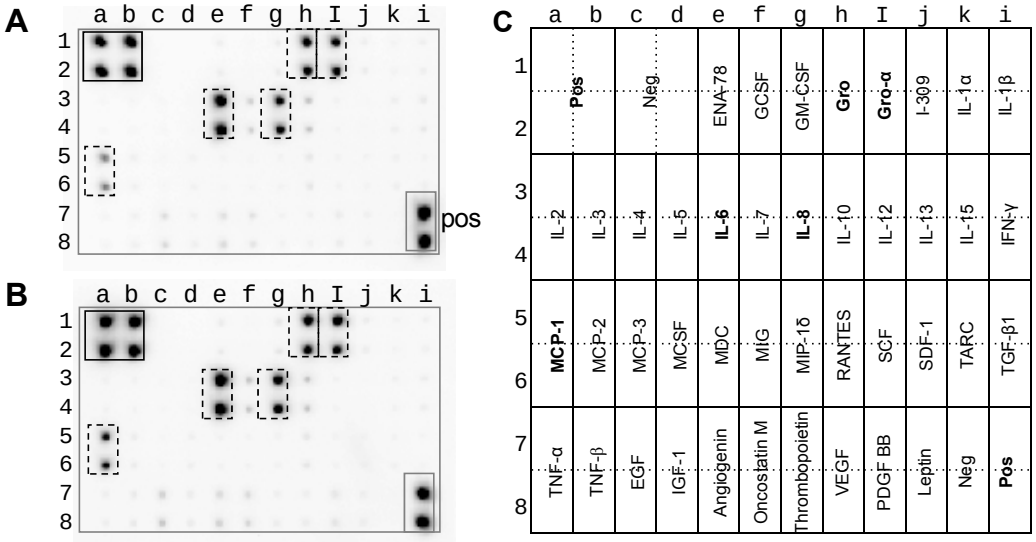

Figure 21. Cytokine array analysis of HBMEC conditioned media.
(A) Array of untreated HBMEC conditioned media. (B) Array of InhA-treated HBMEC conditioned media. (C) Cytokine array map.

InhA induces BBB permeability in vivo.

The *in vitro* results presented above strongly suggest that InhA can induce barrier permeability in HBMEC. To explore whether InhA could actually disrupt the integrity of the BBB *in vivo,* Evans blue (EB) dye extravasation assays in mouse brains were performed after 24, 48 and 72 h post InhA injection through intra-orbital route. The dye was injected into the tail-vein of each mouse 1 hour prior to euthanization (described in the methods section). Digital images were taken immediately after the brains were excised from the body to visualize the amount of dye that penetrated into brain parenchyma (Figure 22). A quantitative measure of the extravasated EB dye extracted from the brain tissues was colorimeterically determined. Measurements were assessed by measuring μg of EB dye per gram of brain. As seen in Figure 23, InhA-treated mice had a significant time-dependent increase in dye uptake by 2-fold compared to control, observed up to 72 h.

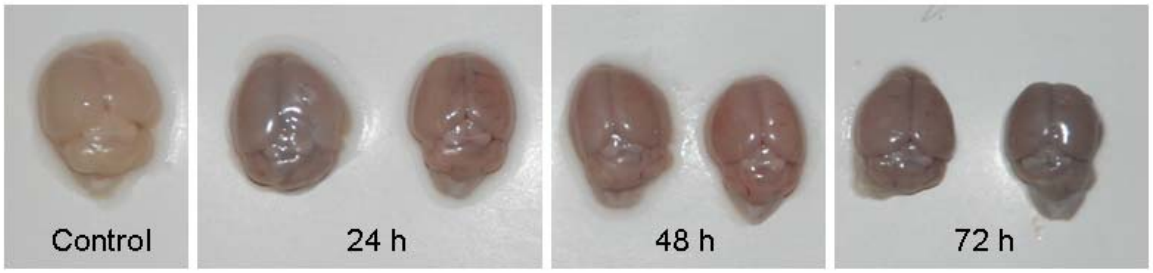

Figure 22. Evans blue extravasation from mice brains in InhA-treated Mice.
BBB vascular permeability was measured as Evans blue dye extravasation from whole mouse brains of control and InhA-treated mice for 24, 48 and 72 h post intraocular injection. Representative pictures of mouse brains were taken of each time point.

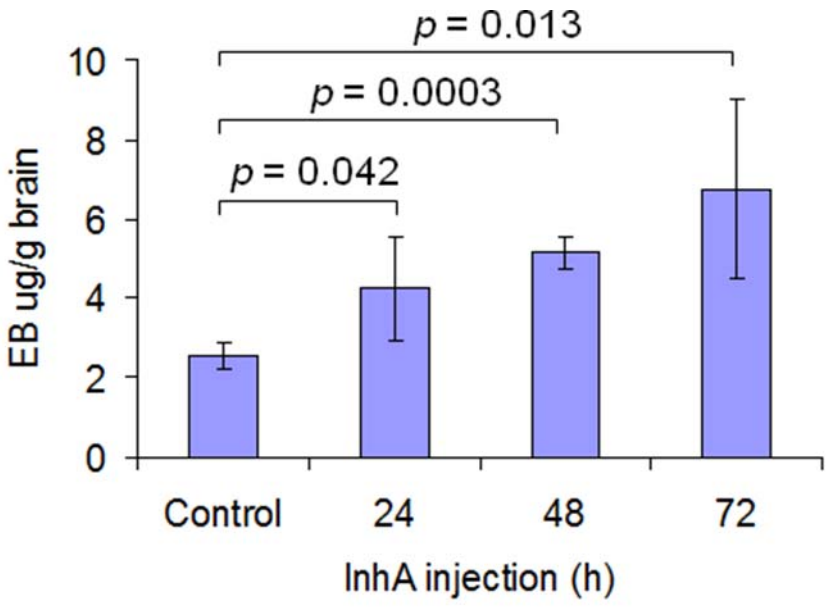

Figure 23. Quantification of EB dye extravasation to the brain.
Control 2.54 µg EB/g brain; at 24 h 4.25 µg EB/ g brain; 48 h 5.14 µg EB/ g brain; 72 h 6.77 µg EB/ g brain. The mean ± SD levels (control n=3, InhA injected groups n = 5) are presented as µg EB dye per gram of brain compared to controls.

Two approaches were taken to establish any possible correlation of the observed InhA effect with anthrax central nervous system pathology as reported earlier (121). Mice injected with fluorescent nanoparticles (Qdots) unconjugated or conjugated to (active and inactive) InhA. Both histological and fluorescence microscopy allowed us to examine this question, as well as to visualize InhA localization within the mouse brain. Histological analysis by bright-field microscopy was done on hematoxylin and esosin (H&E) stained brain tissue sections. Mice treated with either unconjugated nanoparticles (Figure 24A) or heat-inactivated InhA-conjugated nanoparticles (Figure 24B) did not produce any observable pathological changes, thereby eliminating any nonspecific effects of nanoparticles or the trauma of injection. On the other hand, mice treated with

nanoparticles conjugated to active InhA showed considerable leptomeningeal hemorrhaging, thickening, and infiltration of inflammatory cells (Figure 24C and 24D). Hemorrhage was severe enough to affect the brain parenchyma in 20% of these treated mice (Figure 24E and 24F).

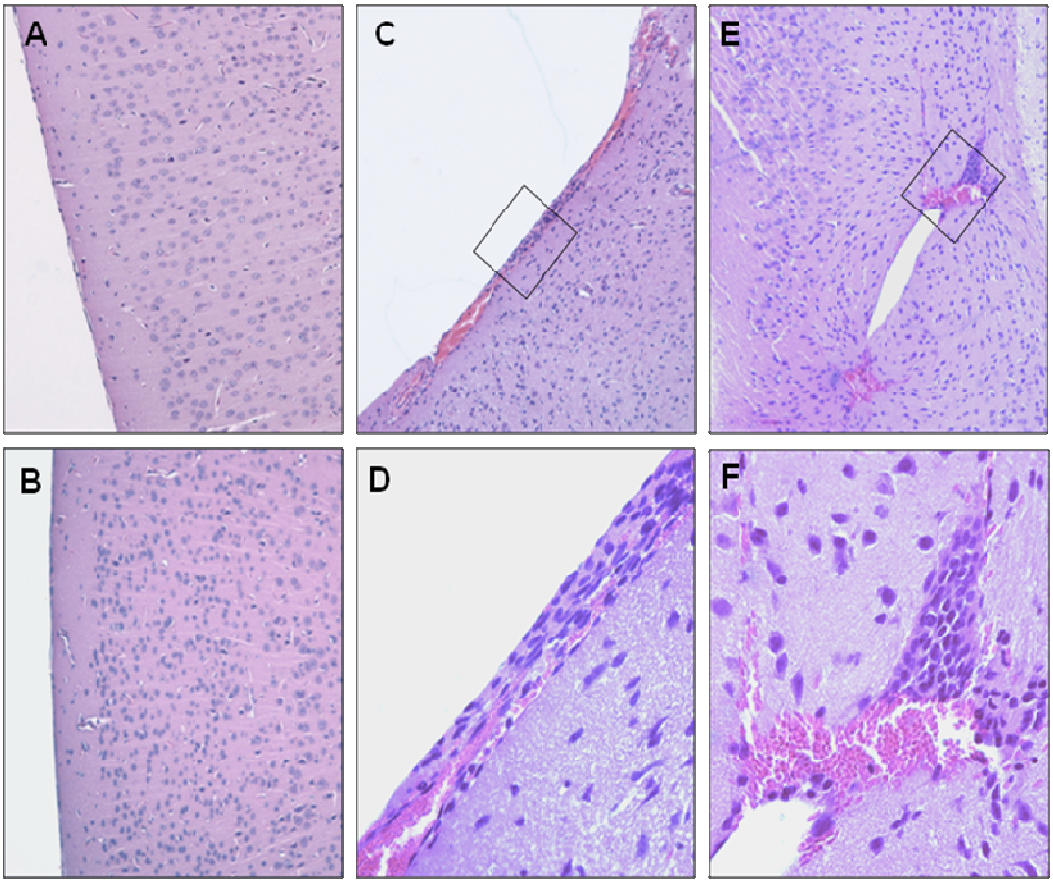

Figure 24. Histopathology of mouse brains.
(A-F) Illustrating histopathology hematoxylin and eosin (H&E) stains of mouse brains (5 micron sections) 24 h after intra-ocular injection with nanoparticles conjugated to (heat-inactivated and active) InhA and nanoparticles alone. (A-D) Displaying meningeal areas. (E,F) Displaying brain parenchyma alone. (A) Mouse brain injected with nanobeads alone. (B) Mouse injected with nanobeads conjugated to heat-inactivated InhA (1 U/ml: 100 µg/ml protein). (C, E) Mouse injected with nanobeads conjugated to active InhA (1 U/ml: 100 µg/ml protein), showing hemorrhagic areas. (D) Enlargement of marked area in C. (F) Enlargement of marked area in E.

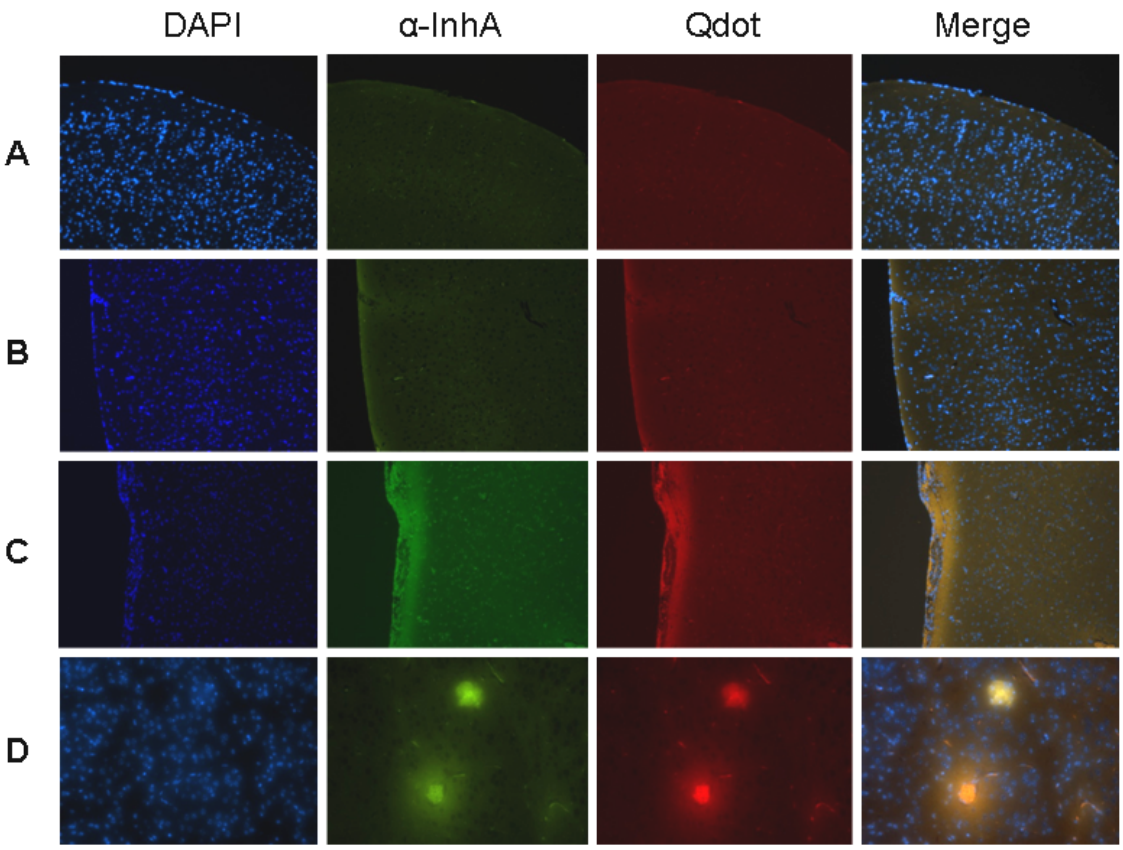

Figure 25. Intravenously (intraocular) administered InhA breaches the BBB and localizes in brain parenchyma after 24 h.
As described in the methods section, immunofluorescence of nanoparticles conjugated to (active and heat-inactive) InhA and immunofluorescence nanoparticles alone were injected intraocularly into the optic sinus. Twenty-four hours later, animals were euthanized and brains were harvested, fixed and prepped for visualization. Five-micron brain sections were immunostained for InhA. Visualization of immunofluorescence nanoparticles (red) and InhA (green) were preformed. (A) Represents sample from mice injected with nanoparticles alone. (B) Mice injected with heat-inactivated InhA conjugated particles. (C, D) Mice injected with active InhA-conjugated nanoparticles. Panels C & D merged show, colocalization of InhA and nanoparticles in brain meningies and brain parenchyma respectively.

Surprisingly, immunofluorescence analysis of similar sections shown in figures 25C and 25D indicates accumulation of active InhA conjugated nanoparticles in the areas corresponding to meningeal thickening and hemorrhage (Figure 24C and 24D). No

prominent fluorescence was detected in the brains of nanoparticles alone and heat-inactivated InhA-conjugated nanoparticles treated mice (Figure 25A, 25B). Collectively, these studies show that InhA is definitely able to breach the BBB of mice and cause hemorrhages, which strongly suggests its role in anthrax meningitis.

5. CONCLUSION

The reported CNS pathology of *B. anthracis* infection leading to hemorrhagic meningitis has drawn our attention to the possible role of some components of these bacteria in the disruption of the blood-brain barrier. Although it has been believed previously that the major virulence factors of anthrax, lethal toxin and edema toxin, play a role in the dissemination and spread of the microbe (121), the massive tissue damage found during the infectious process suggests the possibility of extensive proteolytic activity that may result from bacterial proteases. The finding that the addition of antiprotease-antibiotic treatments of mice infected with *B. anthracis* is able to reduce the mortality and hemorrhages associated with the disease (2) reinforces this possibility.

A presumption that the bacterial toxins might be responsible for disrupting the BBB or BRB needed to be tested. The observations in our TEER experiments on HBMEC and APRE-19 cells using the toxigenic (Sterne) and non-toxigenic (Δ Sterne) strains of *B. anthracis* suggests involvement of additional factors. Since both these strain were found to lower TEER in the monolayers (Figure 7 and 8), production of the toxins by itself may not account for this effect. On the other hand, both Sterne and Δ Sterne strains of *B. anthracis* are known to produce proteases. We undertook the investigation into the role of secreted anthrax proteases on BBB permeability, specifically, metalloprotease InhA and neutral protease Npr599, to get insight into their potential

effects and target molecular components in BBB. Both proteases have been shown to cleave blood coagulation proteins and cell matrix-associated proteins (119; 100). Here we report for the first time a novel property and mechanism of anthrax protease InhA in its ability to induce BBB permeability of HBMEC *in vitro* and in mice *in vivo*.

A marked drop in TEER and morphological changes in HBMECs occurred after treatment with bacterial protease InhA, but not Npr599. These data demonstrate the unique property of the metallo-protease InhA in inducing BBB permeability *in vitro*, while supporting our hypothesis on protease-mediated BBB permeability (Figure 9A and 9B). It was necessary then to investigate how InhA might cause a breach in BBB integrity. Previous studies on TJs have established that the majority of the BBB's barrier- and fence functions and properties can be attributed to the TJ proteins found in HBMEC. Additionally, the alteration of BBB TJ has been implicated in many disease processes of the CNS, particularly in meningitis (46). Therefore, we examined several different TJ proteins for InhA's ability to degrade them; these included Occludin, Claudin-1, JAM-1, and ZO-1. Of the proteins tested, only ZO-1 was found to undergo concentration-dependent cleavage by InhA in HBMEC (Figure 11A and 11B).

The specificity of InhA is quite intriguing, because not only is it unique in its ability for BBB disruption as seen in HBMEC, but also it selectively targets one particular junctional protein, ZO-1. ZO-1 is a membrane-associated guanylate kinase protein that plays a central role in maintaining BBB integrity by anchoring transmembrane TJ proteins and modulation of actin cytoskeleton (132). With these findings we can approach the puzzle about anthrax meningitis, that is, exactly how the

microbes can traverse the BBB. For *B. anthracis* mainly 4 possible routes have been proposed: (a) infecting phagocytes/Trojan horse mechanism (133; 134), (b) transcellular (135; 136), (c) paracellular (137), and (d) non-hematogenous routes (138). A disruption of TJ proteins can ostensibly allow a paracellular migration. However, our further studies into InhA interaction with ZO-1 have provided evidence of an additional or alternative mechanism for *B. anthracis* in crossing the BBB. InhA can directly cleave ZO-1 in naïve cell lysate of HBMECs and recombinant ZO-1 in both concentration-dependent and time-dependent manner. These data suggest that only InhA may gain access into these vascular endothelial cells by a transcellular mechanism, thereby cleaving ZO-1 protein and increasing barrier permeability.

HBMEC are normally non-phagocytic, although under some conditions of injury or infection these cells may become phagocytic (139-142). To check whether InhA can enter the HBMEC, presumably by an endocytic process, we employed eukaryotic inhibitors of phagocytosis. Cytochalasin D, a cell-permeable mycotoxin that inhibits actin polymerization and phagocytosis, and MDC, an inhibitor of endocytosis and trafficking of ligand-receptor complexes through clathrin-coated vesicles, both inhibited InhA-mediated degradation of ZO-1. MDC specifically inhibits transglutaminase, a membrane-associated enzyme that participates in the cross-linking of proteins during clathrin-coated pit formation (128; 143-145). The results with these two eukaryotic inhibitors fairly indicate the partial involvement of endocytosis of InhA, presumably receptor-mediated, in HBMEC. If this process truly occurs, it would mean that InhA

could potentially bind to a putative receptor on the cell surface, became endocytosed, and attack ZO-1 protein intracellularly.

In addition to the effects observed with the endocytosis inhibitors, which indirectly indicate the involvement of InhA endocytosis, we have pursued a functional approach to assessing InhA internalization using HBMEC invasion of (InhA+)-transformed *B. subtilis*. The remarkably higher (24-fold) invasion of these mutants, compared to the InhA-deficient wild-type *B. subtilis* lends further support to InhA internalization in the HBMECs. On the contrary, treatment of B. anthracis spores with anti-InhA antibodies definitively showed a significant reduction in HBMEC invasion. It is remarkable that despite its internalization by endocytosis, InhA itself escapes intracellular degradation, while attacking the target protein (ZO-1). Its resistance to host protease in the phagocytic process may be the key to its success in host cell damage and transmission of the bacteria (130). Our studies on colocalization of InhA with ZO-1 in HBMEC, employing FITC fluorophore further confirm the endocytic process in cell invasion; InhA was found to aggregate towards the periphery of the cell, suggesting potential affinity towards ZO-1.

Some authors recently ascribed the pathological process involved in anthrax meningitis to immuno-suppression through reducing cytokine response (146; 147; 121). InhA proteins are highly conserved across the bacillus species. This protease was first found and isolated from *B. thuringenesis*. The major function of InhA in *B. thuringenesis* is its ability to circumvent the immune system of insects by cleaving lymphatic components in the blood, such as Attacins and Cectopins (148). We could anticipate

encountering these same attributes in an InhA-treated HBMEC culture system. However, secreted cytokine levels did not significantly change after treatment of HBMEC with InhA. Moreover, no cytotoxicity was observed in HBMEC treated with InhA (1 ug/ml) using Alamar blue fluorometric cell viability assay (data not shown). Although there is apparent barrier permeability induced by InhA, the protease itself may not elicit the release of cytokines. It is also feasible that InhA could potentially cleave cytokine proteins similarly as in *B. thuringenesis*. Therefore we hypothesize that InhA might not elicit an immune response.

Firoved et al., 2005 (101) observed that mice treated with edema toxin from *B. anthracis*, developed widespread tissue disruption and focal hemorrhaging; but they did not mention any histopathological lesions in brain meninges. This suggests that the widespread hemorrhage found in anthrax meningitis cannot be explained simply by the actions of the known major virulence factors of anthrax. Notwithstanding these facts, our *in vitro* experiments have convincingly shown that InhA is able to induce barrier permeability in HBMECs. To corroborate these results *in vivo*, we investigated integrity of the BBB in mice after treatment with InhA. Again, our results definitively show that InhA is able to induce BBB permeability. Yet one may ask whether the pathology found during InhA treatment is identical to the pathologies found in anthrax meningitis. Our histopathological observations of brain sections showed thickening of meninges and hemorrhage after treatment with InhA. These results are almost identical to the pathologies displayed in mice infected with anthrax (121). Once again, the similarities in pathology provide strong evidence that InhA could be one of the virulence factors in

anthrax meningitis. With that said, further studies using knock out InhA mutants of anthrax will be necessary to confirm whether InhA's ability to induce barrier permeability and invasion is as effective as its wild-type counterpart.

It has been shown that proteolytic cleavage of cell surface proteins causes activation of host matrix metalloproteases (MMP). In fact, meningitis has been associated with the detection of MMP-9 in tissue samples (149). Since MMP-9 function has been implicated in the regulation of direct cell-cell contacts (150), sections from InhA-treated mice were probed with MMP-9 antibodies to check for any involvement of MMP-9. In these conditions, MMP-9 levels were not detectable; a small fluorescence, if any, was observed in the sections, suggesting a minimal role of host-derived MMP in InhA-induced BBB disruption (data not shown).

We have suggested a novel mechanism involving bacterial processing of a protease that is selectively gets endocytosed by brain endothelial cells, targets a specific TJ proteins of the host cell, disrupts the cell, and yet is apparently resistant to host cell proteases, and by these processes breaches barrier permeability. To date, there are no known pathogens in the BBB that use this method to cross the BBB. Nevertheless, there are pathogens in the enteric system that have similar modes and processes in causing barrier permeability. For example, *Vibrio cholera*, produces a toxin called Zonulin toxin (ZOT) that specifically targets ZO-1 protein for degradation in epithelial cells causing barrier permeability (151). It is interesting to note that a ZOT receptor has been identified in human brain (152). Other bacteria such as *Pseudomonas aeruginosa*, also exclusively target and degrade ZO-1 in epithelial cells, leaving other junctional proteins

intact (153). However, no know cases exist of CNS hemorrhages or meningitis caused by *V. cholera* or *Pseudomonus.* Brain endothelia forming the BBB have distinct structural and functional properties, with rare pinocytosis. Although epithelial cell are fenestrated and do not have the stringent barrier function associated with endothelial cells, further studies on signaling mechanisms involved in ZO-1 degradation in these pathogens may elucidate and shed light on information on our proposed mechanism of InhA in anthrax meningitis.

One of the key features found in clinical autopsies of patients dying of anthrax meningitis is massive hemorrhage, clotting, and swelling of the leptomeninges and intra-parenchyma regions of the brain (154). The phenotypic hemorrhages have been described as "cardinal cap" syndrome because of its bloody appearance (155). Associated features are thrombosis of blood vessels and hemorrhage laden with gram-positive anthrax bacilli (154; 156). Our recent studies have suggested that coagulation and thrombosis induced by *B. anthracis* requires InhA (157). Additionally, another group recently published an article supporting our hypothesis that human blood coagulation takes place in anthrax infection. But specifically, secretion of zinc metalloprotease InhA by anthrax is regulated by the spatial localization and clustering, not the total amount, of bacteria. Then it can be surmised that once bacteria reach areas of the capillaries where they can no longer physically move, secretion of InhA takes place, and as it reaches the threshold level, causes blood coagulation allowing the bacteria to spread to brain parenchyma. These events can pose an additional mechanism for InhA to result in BBB disruption and aggravated hemorrhage.

In studies to characterize potential virulence-associated proteins and vaccine candidates, it has been shown by serological proteome and secretome analysis that InhA is expressed *in vivo* after *B. anthracis* infection. Moreover, moderate levels of immunogenicity were determined by serological protein analysis of InhA (115; 158). Little is known about the actual local levels of secretion of InhA found in relation to meningitis in animals infected with *B. anthracis*. It is important to point out the pathological similarities found in mice treated with InhA and mice infected with anthrax (94; 121). Although the mice did not die from the injection of InhA, several factors need consideration. First, the dosage chosen for InhA is far less than dosages for other toxins used in anthrax studies (101; 94; 121). Secondly, given the fact we only injected a fixed amount of the protease, many different inhibitors and counteracting agents contained in the blood may neutralize or reduce the effect seen, thereby not causing death in mice. Therefore, the optimal lethal effect can be attained when the bacteria are present in sufficient amounts to consistently produce the enzyme. Obviously it is not possible to determine how much InhA is secreted at the BBB in an infection; answering this would require a different experimental approach, to directly and causally relate our findings with anthrax meningitis.

In conclusion, we reported here InhA-induced BBB disruption provides a mechanistic model for human hemorrhagic anthrax meningitis. We have definitively identified a protease, its primary substrate, and its unique cell invasion process in the closely structured human brain endothelia. The results of our various *in vitro* experiments on the model cells, HBMEC, as well as of *in vivo* observations in mice lead us to the

inescapable conclusion that this particular metalloprotease invades the endothelial cells, attacking primarily the TJ protein ZO-1, and ultimately causing hemorrhage in the meninges. This evidence adds a new dimension to our understanding of hemorrhagic meningitis in anthrax infections. InhA may be the major pathogenic factor, and so can be an important molecular target for preventive therapy against fatal hemorrhages associated with *B. anthracis* infection.

We are aware, of course, that this may be only the beginning of a many further questions for future investigation. It is obviously not possible to attribute the entire causal role in anthrax-induced meningo-encephalitis to the *B. anthracis*-secreted metalloprotease InhA, since the final fate or the end-products of this protease is not yet determined. In the overall consideration, it is interesting to note that these bacilli secrete a product that, like an emissary, aims at the cerebral vascular tight junction, gets endocytosed, escapes being degraded by the host cell's phagolysosomal enzymes, then targets and degrades the key junctional protein, Zonulin, and co-localizes near the cell nucleus. Is it going to affect and alter the genome or its transcription factors, one may ask? However, that is not required for disrupting the BBB, and thus, inducing permeability. What other effects the anthrax bacilli may exert in the CNS parenchyma is not known, and also is beyond the scope of our main research objective. However, we have not found evidence of inflammatory reaction products, *e.g.*, cytokines, in the HBMEC, as is usual with most bacterial invasions of tissue and septicemia.

In a larger context of the systemic effects of *B. anthracis* infection it is quite likely that InhA may be causally related to other tissue injuries through disruption of the

tight junctions where zonulin occurs, as we have seen with the CNS vascular endothelial cells (HBMEC). Our evidence amply demonstrates that the critical step in BBB disruption is accomplished by InhA through utilizing a major part of the host endothelia's own signaling apparatus. Future research to corroborate our conclusions will need to pursue whether the endothelial TJ's carry specific receptors for InhA, comparable, for example, to the ZOT receptors discussed above, and if so, then these components should be identified and functionally characterized. Secondly, InhA's likely association with the host cells' signaling and counter-regulatory pathways needs to be identified. Finally, a gene knockout model of *B. anthracis* can ultimately confirm the purported role of anthrax-secreted InhA in BBB disruption and meningitis that our studies have established.

REFERENCES

REFERENCES

1. Kim KS. Pathogenesis of bacterial meningitis: from bacteraemia to neuronal injury. Nat Rev Neurosci. 2003 May ;4(5):376-85.

2. Popov SG, Popova TG, Hopkins S, Weinstein RS, MacAfee R, Fryxell KJ, Chandhoke V, Bailey C, Alibek K. Effective antiprotease-antibiotic treatment of experimental anthrax. BMC Infect Dis. 2005 ;5(1):25.

3. Dirckx JH. Virgil on anthrax. Am J Dermatopathol. 1981 ;3(2):191-5.

4. Riedel S. Anthrax: a continuing concern in the era of bioterrorism. Proc (Bayl Univ Med Cent). 2005 Jul ;18(3):234-43.

5. Kohout E, Sehats A, Ashraf M. Anthrax: a continous problem in southwest Iran. Am J Med Sci. 1964 May ;247:565-75.

6. Summary of notifiable diseases, United States 1994. MMWR Morb Mortal Wkly Rep. 1994 ;43(53):1-80.

7. Carter KC. The Koch-Pasteur dispute on establishing the cause of anthrax. Bull Hist Med. 1988 ;62(1):42-57.

8. Sternbach G. The history of anthrax. J Emerg Med. 2003 May ;24(4):463-7.

9. Turnbull PC. Definitive identification of Bacillus anthracis--a review. J Appl Microbiol. 1999 Aug ;87(2):237-40.

10. Spencer RC. Bacillus anthracis. J Clin Pathol. 2003 Mar 1;56(3):182-187.

11. Uchida I, Sekizaki T, Hashimoto K, Terakado N. Association of the encapsulation of Bacillus anthracis with a 60 megadalton plasmid. J Gen Microbiol. 1985 Feb ;131(2):363-7.

12. Leppla SH. Anthrax toxin edema factor: a bacterial adenylate cyclase that increases cyclic AMP concentrations of eukaryotic cells. Proc Natl Acad Sci U S A. 1982 May ;79(10):3162-6.

13. Leppla SH. Bacillus anthracis calmodulin-dependent adenylate cyclase: chemical and enzymatic properties and interactions with eucaryotic cells. Adv Cyclic Nucleotide Protein Phosphorylation Res. 1984 ;17189-98.

14. O'Brien J, Friedlander A, Dreier T, Ezzell J, Leppla S. Effects of anthrax toxin components on human neutrophils. Infect Immun. 1985 Jan ;47(1):306-10.

15. Baldari CT, Tonello F, Paccani SR, Montecucco C. Anthrax toxins: A paradigm of bacterial immune suppression. Trends Immunol. 2006 Sep ;27(9):434-40.

16. Mogridge J, Cunningham K, Lacy DB, Mourez M, Collier RJ. The lethal and edema factors of anthrax toxin bind only to oligomeric forms of the protective antigen. Proc Natl Acad Sci U S A. 2002 May 14;99(10):7045-8.

17. Young JA, Collier RJ. Anthrax toxin: receptor binding, internalization, pore formation, and translocation. Annu Rev Biochem. 2007 ;76:243-65.

18. Friedlander AM, Welkos SL, Pitt ML, Ezzell JW, Worsham PL, Rose KJ, Ivins BE, Lowe JR, Howe GB, Mikesell P. Postexposure prophylaxis against experimental inhalation anthrax. J Infect Dis. 1993 May ;167(5):1239-43.

19. Turner M. Anthrax in humans in Zimbabwe. Cent Afr J Med. 1980 Jul ;26(7):160-1.

20. Lew D. Principles and Practice of Infectious Diseases. 4th ed. New York: Churchhill Livingstone; 1995.

21. Kunanusont C, Limpakarnjanarat K, Foy HM. Outbreak of anthrax in Thailand. Ann Trop Med Parasitol. 1990 Oct ;84(5):507-12.

22. Sirisanthana T, Navachareon N, Tharavichitkul P, Sirisanthana V, Brown AE. Outbreak of oral-oropharyngeal anthrax: an unusual manifestation of human infection with Bacillus anthracis. Am J Trop Med Hyg. 1984 Jan ;33(1):144-50.

23. Albrink WS, Brooks SM, Biron RE, Kopel M. Human inhalation anthrax. A report of three fatal cases. Am J Pathol. 1960 Apr ;36:457-71.

24. Plotkin SA, Brachman PS, Utell M, Bumford FH, Atchison MM. An epidemic of inhalation anthrax, the first in the twentieth century: I. Clinical features. 1960. Am J Med. 2002 Jan ;112(1):4-12; discussion 2-3.

25. Inglesby TV, O'Toole T, Henderson DA, Bartlett JG, Ascher MS, Eitzen E, Friedlander AM, Gerberding J, Hauer J, Hughes J, McDade J, Osterholm MT, Parker G, Perl TM, Russell PK, Tonat K. Anthrax as a biological weapon, 2002: updated recommendations for management. JAMA. 2002 May 1;287(17):2236-52.

26. Lanska DJ. Anthrax meningoencephalitis. Neurology. 2002 Aug 13;59(3):327-34.

27. MacIntyre A, Hammond CJ, Little CS, Appelt DM, Balin BJ. Chlamydia pneumoniae infection alters the junctional complex proteins of human brain microvascular endothelial cells. FEMS Microbiol Lett. 2002 Dec 17;217(2):167-72.

28. Sheedlo HJ, Li L, Turner JE. Effects of RPE-cell factors secreted from permselective fibers on retinal cells in vitro. Brain Res. 1992 Aug 7;587(2):327-37.

29. Bok D. The retinal pigment epithelium: a versatile partner in vision. J Cell Sci Suppl. 1993 ;17:189-95.

30. Giordano GG, Thomson RC, Ishaug SL, Mikos AG, Cumber S, Garcia CA, Lahiri-Munir D. Retinal pigment epithelium cells cultured on synthetic biodegradable polymers. J Biomed Mater Res. 1997 Jan ;34(1):87-93.

31. Bailey TA, Kanuga N, Romero IA, Greenwood J, Luthert PJ, Cheetham ME. Oxidative stress affects the junctional integrity of retinal pigment epithelial cells. Invest Ophthalmol Vis Sci. 2004 Feb ;45(2):675-84.

32. Toimela T, Mäenpää H, Mannerström M, Tähti H. Development of an in vitro blood-brain barrier model-cytotoxicity of mercury and aluminum. Toxicol Appl Pharmacol. 2004 Feb 15;195(1):73-82.

33. Tuomanen EI. Entry of pathogens into the central nervous system. FEMS Microbiol Rev. 1996 Jul ;18(4):289-99.

34. Schlosshauer B. The blood-brain barrier: morphology, molecules, and neurothelin. Bioessays. 1993 May ;15(5):341-6.

35. Marcial MA, Carlson SL, Madara JL. Partitioning of paracellular conductance along the ileal crypt-villus axis: a hypothesis based on structural analysis with detailed consideration of tight junction structure-function relationships. J Membr Biol. 1984 ;80(1):59-70.

36. Nagy Z, Peters H, Hüttner I. Fracture faces of cell junctions in cerebral endothelium during normal and hyperosmotic conditions. Lab Invest. 1984 Mar ;50(3):313-22.

37. Schütze S, Machleidt T, Adam D, Schwandner R, Wiegmann K, Kruse ML, Heinrich M, Wickel M, Krönke M. Inhibition of receptor internalization by monodansylcadaverine selectively blocks p55 tumor necrosis factor receptor death domain signaling. J Biol Chem. 1999 Apr 9;274(15):10203-12.

38. Schulze C, Firth JA. Immunohistochemical localization of adherens junction components in blood-brain barrier microvessels of the rat. J Cell Sci. 1993 Mar ;104 (Pt 3)773-82.

39. Kniesel U, Wolburg H. Tight junctions of the blood-brain barrier. Cell Mol Neurobiol. 2000 Feb ;20(1):57-76.

40. Lane NJ, Reese TS, Kachar B. Structural domains of the tight junctional intramembrane fibrils. Tissue Cell. 1992 ;24(2):291-300.

41. Suzuki F, Nagano T. Three-dimensional model of tight junction fibrils based on freeze-fracture images. Cell Tissue Res. 1991 May ;264(2):381-4.

42. Hüttner I, Peters H. Heterogeneity of cell junctions in rat aortic endothelium: a freeze-fracture study. J Ultrastruct Res. 1978 Sep ;64(3):303-8.

43. Simionescu M, Simionescu N, Palade GE. Segmental differentiations of cell junctions in the vascular endothelium. Arteries and veins. J Cell Biol. 1976 Mar ;68(3):705-23.

44. Møllgård K, Saunders NR. The development of the human blood-brain and blood-CSF barriers. Neuropathol Appl Neurobiol. 1986 ;12(4):337-58.

45. Vincent PA, Xiao K, Buckley KM, Kowalczyk AP. VE-cadherin: adhesion at arm's length. Am J Physiol Cell Physiol. 2004 May ;286(5):C987-97.

46. Hawkins BT, Davis TP. The blood-brain barrier/neurovascular unit in health and disease. Pharmacol Rev. 2005 Jun ;57(2):173-85.

47. Dejana E, Lampugnani MG, Martinez-Estrada O, Bazzoni G. The molecular organization of endothelial junctions and their functional role in vascular morphogenesis and permeability. Int J Dev Biol. 2000 ;44(6):743-8.

48. Morcos Y, Hosie MJ, Bauer HC, Chan-Ling T. Immunolocalization of occludin and claudin-1 to tight junctions in intact CNS vessels of mammalian retina. J Neurocytol. 2001 Feb ;30(2):107-23.

49. Nitta T, Hata M, Gotoh S, Seo Y, Sasaki H, Hashimoto N, Furuse M, Tsukita S. Size-selective loosening of the blood-brain barrier in claudin-5-deficient mice. J Cell Biol. 2003 May 12;161(3):653-60.

50. Wolburg H, Wolburg-Buchholz K, Kraus J, Rascher-Eggstein G, Liebner S, Hamm S, Duffner F, Grote E, Risau W, Engelhardt B. Localization of claudin-3 in tight junctions of the blood-brain barrier is selectively lost during experimental autoimmune encephalomyelitis and human glioblastoma multiforme. Acta Neuropathol. 2003 Jun ;105(6):586-92.

51. Dejana E. Endothelial cell-cell junctions: happy together. Nat Rev Mol Cell Biol. 2004 Apr ;5(4):261-70.

52. Howarth AG, Hughes MR, Stevenson BR. Detection of the tight junction-associated protein ZO-1 in astrocytes and other nonepithelial cell types. Am J Physiol. 1992 Feb ;262(2 Pt 1):C461-9.

53. Stevenson BR, Siliciano JD, Mooseker MS, Goodenough DA. Identification of ZO-1: a high molecular weight polypeptide associated with the tight junction (zonula occludens) in a variety of epithelia. J Cell Biol. 1986 Sep ;103(3):755-66.

54. Wolburg H, Lippoldt A. Tight junctions of the blood-brain barrier: development, composition and regulation. Vascul Pharmacol. 2002 Jun ;38(6):323-37.

55. González-Mariscal L, Betanzos A, Avila-Flores A. MAGUK proteins: structure and role in the tight junction. Semin Cell Dev Biol. 2000 Aug ;11(4):315-24.

56. Fischer S, Wobben M, Marti HH, Renz D, Schaper W. Hypoxia-induced hyperpermeability in brain microvessel endothelial cells involves VEGF-mediated changes in the expression of zonula occludens-1. Microvasc Res. 2002 Jan ;63(1):70-80.

57. Balda M, Gonzalez-Mariscal L, Matter K, Cereijido M, Anderson J. Assembly of the tight junction: the role of diacylglycerol. J. Cell Biol. 1993 Oct 1;123(2):293-302.

58. Betanzos A, Huerta M, Lopez-Bayghen E, Azuara E, Amerena J, González-Mariscal L. The tight junction protein ZO-2 associates with Jun, Fos and C/EBP transcription factors in epithelial cells. Exp Cell Res. 2004 Jan 1;292(1):51-66.

59. Islas S, Vega J, Ponce L, González-Mariscal L. Nuclear localization of the tight junction protein ZO-2 in epithelial cells. Exp Cell Res. 2002 Mar 10;274(1):138-48.

60. Traweger A, Fuchs R, Krizbai IA, Weiger TM, Bauer H, Bauer H. The tight junction protein ZO-2 localizes to the nucleus and interacts with the heterogeneous nuclear ribonucleoprotein scaffold attachment factor-B. J Biol Chem. 2003 Jan 24;278(4):2692-700.

61. Itoh M, Morita K, Tsukita S. Characterization of ZO-2 as a MAGUK Family Member Associated with Tight as well as Adherens Junctions with a Binding Affinity to Occludin and alpha-Catenin. J. Biol. Chem. 1999 Feb 26;274(9):5981-86.

62. Inoko A, Itoh M, Tamura A, Matsuda M, Furuse M, Tsukita S. Expression and distribution of ZO-3, a tight junction MAGUK protein, in mouse tissues. Genes to Cells. 2003 Nov 1;8(11):837-845.

63. Sawada N, Murata M, Kikuchi K, Osanai M, Tobioka H, Kojima T, Chiba H. Tight junctions and human diseases. Med Electron Microsc. 2003 Sep ;36(3):147-56.

64. Citi S, Sabanay H, Kendrick-Jones J, Geiger B. Cingulin: characterization and localization. J Cell Sci. 1989 May 1;93(1):107-22.

65. Yamamoto T, Harada N, Kawano Y, Taya S, Kaibuchi K. In vivo interaction of AF-6 with activated Ras and ZO-1. Biochem Biophys Res Commun. 1999 May 27;259(1):103-7.

66. Adamson P, Wilbourn B, Etienne-Manneville S, Calder V, Beraud E, Milligan G, Couraud P, Greenwood J. Lymphocyte trafficking through the blood-brain barrier is dependent on endothelial cell heterotrimeric G-protein signaling. FASEB J. 2002 Aug ;16(10):1185-94.

67. Fábián G, Szabó CA, Bozó B, Greenwood J, Adamson P, Deli MA, Joó F, Krizbai IA, Szucs M. Expression of G-protein subtypes in cultured cerebral endothelial cells. Neurochem Int. 1998 Aug ;33(2):179-85.

68. Hopkins AM, Li D, Mrsny RJ, Walsh SV, Nusrat A. Modulation of tight junction function by G protein-coupled events. Adv Drug Deliv Rev. 2000 Jun 30;41(3):329-40.

69. Saha C, Nigam SK, Denker BM. Involvement of Galphai2 in the maintenance and biogenesis of epithelial cell tight junctions. J Biol Chem. 1998 Aug 21;273(34):21629-33.

70. Andreeva AY, Krause E, Müller EC, Blasig IE, Utepbergenov DI. Protein kinase C regulates the phosphorylation and cellular localization of occludin. J Biol Chem. 2001 Oct 19;276(42):38480-6.

71. Kurihara H, Anderson JM, Farquhar MG. Increased Tyr phosphorylation of ZO-1 during modification of tight junctions between glomerular foot processes. Am J Physiol. 1995 Mar ;268(3 Pt 2):F514-24.

72. Stevenson BR, Anderson JM, Braun ID, Mooseker MS. Phosphorylation of the tight-junction protein ZO-1 in two strains of Madin-Darby canine kidney cells which differ in transepithelial resistance. Biochem J. 1989 Oct 15;263(2):597-9.

73. Sakakibara A, Furuse M, Saitou M, Ando-Akatsuka Y, Tsukita S. Possible involvement of phosphorylation of occludin in tight junction formation. J Cell Biol. 1997 Jun 16;137(6):1393-401.

74. Nagy Z, Goehlert UG, Wolfe LS, Hüttner I. Ca2+ depletion-induced disconnection of tight junctions in isolated rat brain microvessels. Acta Neuropathol. 1985 ;68(1):48-52.

75. Abbott NJ, Revest PA. Control of brain endothelial permeability. Cerebrovasc Brain Metab Rev. 1991 ;3(1):39-72.

76. Brown RC, Davis TP. Hypoxia/aglycemia alters expression of occludin and actin in brain endothelial cells. Biochem Biophys Res Commun. 2005 Feb 25;327(4):1114-23.

77. Lippoldt A, Kniesel U, Liebner S, Kalbacher H, Kirsch T, Wolburg H, Haller H. Structural alterations of tight junctions are associated with loss of polarity in stroke-prone spontaneously hypertensive rat blood-brain barrier endothelial cells. Brain Res. 2000 Dec 8;885(2):251-61.

78. Goldstein LB, Adams R, Becker K, Furberg CD, Gorelick PB, Hademenos G, Hill M, Howard G, Howard VJ, Jacobs B, Levine SR, Mosca L, Sacco RL, Sherman DG, Wolf PA, del Zoppo GJ. Primary prevention of ischemic stroke: A statement for healthcare professionals from the Stroke Council of the American Heart Association. Stroke. 2001 Jan ;32(1):280-99.

79. Engelhardt B. The blood–brain barrier. Wiley; 1997.

80. Lassmann H. Comparative neuropathology of chronic experimental allergic encephalomyelitis and multiple sclerosis. Schriftenr Neurol. 1983 ;251-135.

81. Long DM. Capillary ultrastructure and the blood-brain barrier in human malignant brain tumors. J Neurosurg. 1970 Feb ;32(2):127-44.

82. Fischer S, Clauss M, Wiesnet M, Renz D, Schaper W, Karliczek GF. Hypoxia induces permeability in brain microvessel endothelial cells via VEGF and NO. Am J Physiol. 1999 Apr ;276(4 Pt 1):C812-20.

83. Mark KS, Burroughs AR, Brown RC, Huber JD, Davis TP. Nitric oxide mediates hypoxia-induced changes in paracellular permeability of cerebral microvasculature. Am J Physiol Heart Circ Physiol. 2004 Jan ;286(1):H174-80.

84. Coomber BL, Stewart PA, Hayakawa K, Farrell CL, Del Maestro RF. Quantitative morphology of human glioblastoma multiforme microvessels: structural basis of blood-brain barrier defect. J Neurooncol. 1987 ;5(4):299-307.

85. Hoover KB, Liao SY, Bryant PJ. Loss of the tight junction MAGUK ZO-1 in breast cancer: relationship to glandular differentiation and loss of heterozygosity. Am J Pathol. 1998 Dec ;153(6):1767-73.

86. Woods DF, Bryant PJ. The discs-large tumor suppressor gene of Drosophila encodes a guanylate kinase homolog localized at septate junctions. Cell. 1991 Aug 9;66(3):451-64.

87. Turner G. Cerebral Malaria. Brain Pathology. 1997 ;7(1):569-82.

88. Quagliarello VJ, Wispelwey B, Jr WJL, Scheld WM. Recombinant human interleukin-1 induces meningitis and blood-brain barrier injury in the rat. Characterization and comparison with tumor necrosis factor. J Clin Invest. . 1991 Apr ;87(4):1360–66.

89. Cundell DR, Gerard NP, Gerard C, Idanpaan-Heikkila I, Tuomanen EI. Streptococcus pneumoniae anchor to activated human cells by the receptor for platelet-activating factor. Nature. 1995 Oct 5;377(6548):435-38.

90. Mark KS, Davis TP. Cerebral microvascular changes in permeability and tight junctions induced by hypoxia-reoxygenation. Am J Physiol Heart Circ Physiol. 2002 Apr ;282(4):H1485-94.

91. Friedlander AM. Anthrax: clinical features, pathogenesis, and potential biological warfare threat. Curr Clin Top Infect Dis. 2000 ;20335-49.

92. Hanna P. Lethal toxin actions and their consequences. J Appl Microbiol. 1999 Aug ;87(2):285-7.

93. Moayeri M, Leppla SH. The roles of anthrax toxin in pathogenesis. Curr Opin Microbiol. 2004 Feb ;7(1):19-24.

94. Moayeri M, Haines D, Young HA, Leppla SH. Bacillus anthracis lethal toxin induces TNF-alpha-independent hypoxia-mediated toxicity in mice. J Clin Invest. 2003 Sep ;112(5):670-82.

95. Fang H, Cordoba-Rodriguez R, Lankford CSR, Frucht DM. Anthrax lethal toxin blocks MAPK kinase-dependent IL-2 production in CD4+ T cells. J Immunol. 2005 Apr 15;174(8):4966-71.

96. Fukao T. Immune system paralysis by anthrax lethal toxin: the roles of innate and adaptive immunity. Lancet Infect Dis. 2004 Mar ;4(3):166-70.

97. Guidi-Rontani C. The alveolar macrophage: the Trojan horse of Bacillus anthracis. Trends Microbiol. 2002 Sep ;10(9):405-9.

98. Popov SG, Villasmil R, Bernardi J, Grene E, Cardwell J, Popova T, Wu A, Alibek D, Bailey C, Alibek K. Effect of Bacillus anthracis lethal toxin on human peripheral blood mononuclear cells. FEBS Lett. 2002 Sep 11;527(1-3):211-5.

99. Warfel JM, Steele AD, D'Agnillo F. Anthrax lethal toxin induces endothelial barrier dysfunction. Am J Pathol. 2005 Jun ;166(6):1871-81.

100. Chung M, Popova TG, Millis BA, Mukherjee DV, Zhou W, Liotta LA, Petricoin EF, Chandhoke V, Bailey C, Popov SG. Secreted neutral metalloproteases of Bacillus anthracis as candidate pathogenic factors. J Biol Chem. 2006 Oct 20;281(42):31408-18.

101. Firoved AM, Miller GF, Moayeri M, Kakkar R, Shen Y, Wiggins JF, McNally EM, Tang W, Leppla SH. Bacillus anthracis edema toxin causes extensive tissue lesions and rapid lethality in mice. Am J Pathol. 2005 Nov ;167(5):1309-20.

102. Abramova FA, Grinberg LM, Yampolskaya OV, Walker DH. Pathology of inhalational anthrax in 42 cases from the Sverdlovsk outbreak of 1979. Proc Natl Acad Sci U S A. 1993 Mar 15;90(6):2291-4.

103. Grinberg LM, Abramova FA, Yampolskaya OV, Walker DH, Smith JH. Quantitative pathology of inhalational anthrax I: quantitative microscopic findings. Mod Pathol. 2001 May ;14(5):482-95.

104. Vasconcelos D, Barnewall R, Babin M, Hunt R, Estep J, Nielsen C, Carnes R, Carney J. Pathology of inhalation anthrax in cynomolgus monkeys (Macaca fascicularis). Lab Invest. 2003 Aug ;83(8):1201-9.

105. Smith H, Keppie J. Observations on experimental anthrax; demonstration of a specific lethal factor produced in vivo by Bacillus anthracis. Nature. 1954 May 8;173(4410):869-70.

106. Smith JH, Keppie J, Stanley JL. The chemical basis of the virulence of Bacillus anthracis. V. The specific toxin produced by B. Anthracis in vivo. Br J Exp Pathol. 1955 Oct ;36(5):460-72.

107. Friedlander AM. Tackling anthrax. Nature. 2001 Nov 8;414(6860):160-1.

108. Cui X, Moayeri M, Li Y, Li X, Haley M, Fitz Y, Correa-Araujo R, Banks SM, Leppla SH, Eichacker PQ. Lethality during continuous anthrax lethal toxin infusion is associated with circulatory shock but not inflammatory cytokine or nitric oxide release in rats. Am J Physiol Regul Integr Comp Physiol. 2004 Apr ;286(4):R699-709.

109. Read TD, Peterson SN, Tourasse N, Baillie LW, Paulsen IT, Nelson KE, Tettelin H, Fouts DE, Eisen JA, Gill SR, Holtzapple EK, Okstad OA, Helgason E, Rilstone J, Wu M, Kolonay JF, Beanan MJ, Dodson RJ, Brinkac LM, Gwinn M, DeBoy RT, Madpu R, Daugherty SC, Durkin AS, Haft DH, Nelson WC, Peterson JD, Pop M, Khouri HM, Radune D, Benton JL, Mahamoud Y, Jiang L, Hance IR, Weidman JF, Berry KJ, Plaut RD, Wolf AM, Watkins KL, Nierman WC, Hazen A, Cline R, Redmond C, Thwaite JE, White O, Salzberg SL, Thomason B, Friedlander AM, Koehler TM, Hanna PC, Kolstø A, Fraser CM. The genome sequence of Bacillus anthracis Ames and comparison to closely related bacteria. Nature. 2003 May 1;423(6935):81-6.

110. Miyoshi S, Nakazawa H, Kawata K, Tomochika K, Tobe K, Shinoda S. Characterization of the hemorrhagic reaction caused by Vibrio vulnificus metalloprotease, a member of the thermolysin family. Infect Immun. 1998 Oct ;66(10):4851-5.

111. Okamoto T, Akaike T, Suga M, Tanase S, Horie H, Miyajima S, Ando M, Ichinose Y, Maeda H. Activation of human matrix metalloproteinases by various bacterial proteinases. J Biol Chem. 1997 Feb 28;272(9):6059-66.

112. Sakata Y, Akaike T, Suga M, Ijiri S, Ando M, Maeda H. Bradykinin generation triggered by Pseudomonas proteases facilitates invasion of the systemic circulation by Pseudomonas aeruginosa. Microbiol Immunol. 1996 ;40(6):415-23.

113. Shin YH, Akaike T, Khan MM, Sakata Y, Maeda H. Further evidence of bradykinin involvement in septic shock: reduction of kinin production in vivo and improved survival in rats by use of polymer tailored SBTI with longer t1/2. Immunopharmacology. 1996 Jun ;33(1-3):369-73.

114. Supuran CT, Scozzafava A, Clare BW. Bacterial protease inhibitors. Medicinal Research Reviews. 2002 ;22(4):329-72.

115. Ariel N, Zvi A, Makarova KS, Chitlaru T, Elhanany E, Velan B, Cohen S, Friedlander AM, Shafferman A. Genome-based bioinformatic selection of chromosomal Bacillus anthracis putative vaccine candidates coupled with proteomic identification of surface-associated antigens. Infect Immun. 2003 Aug ;71(8):4563-79.

116. Badger JL, Stins MF, Kim KS. Citrobacter freundii invades and replicates in human brain microvascular endothelial cells. Infect Immun. 1999 Aug ;67(8):4208-15.

117. Huang SH, Stins MF, Kim KS. Bacterial penetration across the blood-brain barrier during the development of neonatal meningitis. Microbes Infect. 2000 Aug ;2(10):1237-44.

118. Stins MF, Gilles F, Kim KS. Selective expression of adhesion molecules on human brain microvascular endothelial cells. J Neuroimmunol. 1997 Jun ;76(1-2):81-90.

119. Chung M, Popova TG, Jorgensen SC, Dong L, Chandhoke V, Bailey CL, Popov SG. Degradation of circulating von Willebrand factor and its regulator ADAMTS13 implicates secreted Bacillus anthracis metalloproteases in anthrax consumptive coagulopathy. J Biol Chem. 2008 Apr 11;283(15):9531-42.

120. Treeratanapiboon L, Psathaki K, Wegener J, Looareesuwan S, Galla H, Udomsangpetch R. In vitro study of malaria parasite induced disruption of blood-brain barrier. Biochem Biophys Res Commun. 2005 Sep 30;335(3):810-8.

121. van Sorge NM, Ebrahimi CM, McGillivray SM, Quach D, Sabet M, Guiney DG, Doran KS. Anthrax toxins inhibit neutrophil signaling pathways in brain endothelium and contribute to the pathogenesis of meningitis. PLoS ONE. 2008 ;3(8):e2964.

122. Egima CM, Macedo SF, Sasso GR, Covarrubias C, Cortez M, Maeda FY, Costa FT, Yoshida N. Co-infection with Trypanosoma cruzi protects mice against early death by neurological or pulmonary disorders induced by Plasmodium berghei ANKA. Malar J. 2007 ;690.

123. Yepes M, Sandkvist M, Moore EG, Bugge TH, Strickland DK, Lawrence DA. Tissue-type plasminogen activator induces opening of the blood-brain barrier via the LDL receptor-related protein. J. Clin. Invest. . 2003 Nov ;112(10):1533-1540.

124. Mitic LL, Anderson JM. Molecular architecture of tight junctions. Annu Rev Physiol. 1998 ;60:121-42.

125. Stevenson BR, Keon BH. The tight junction: morphology to molecules. Annu Rev Cell Dev Biol. 1998 ;14:89-109.

126. Tsukita S, Furuse M, Itoh M. Multifunctional strands in tight junctions. Nat Rev Mol Cell Biol. 2001 Apr ;2(4):285-93.

127. Tanenbaum SW. Cytochalasins: biochemical and cell biological aspects. New York, N.Y.: North-Holland; 1978.

128. Davies PJ, Davies DR, Levitzki A, Maxfield FR, Milhaud P, Willingham MC, Pastan IH. Transglutaminase is essential in receptor-mediated endocytosis of alpha 2-macroglobulin and polypeptide hormones. Nature. 1980 Jan 10;283(5743):162-7.

129. Larkin JM, Brown MS, Goldstein JL, Anderson RG. Depletion of intracellular potassium arrests coated pit formation and receptor-mediated endocytosis in fibroblasts. Cell. 1983 May ;33(1):273-85.

130. Ramarao N, Lereclus D. The InhA1 metalloprotease allows spores of the B. cereus group to escape macrophages. Cell Microbiol. 2005 Sep ;7(9):1357-64.

131. Charlton S, Moir AJ, Baillie L, Moir A. Characterization of the exosporium of Bacillus cereus. J Appl Microbiol. 1999 Aug ;87(2):241-5.

132. Harhaj NS, Antonetti DA. Regulation of tight junctions and loss of barrier function in pathophysiology. Int J Biochem Cell Biol. 2004 Jul ;36(7):1206-37.

133. Drevets DA, Leenen PJM, Greenfield RA. Invasion of the central nervous system by intracellular bacteria. Clin Microbiol Rev. 2004 Apr ;17(2):323-47.

134. Join-Lambert OF, Ezine S, Le Monnier A, Jaubert F, Okabe M, Berche P, Kayal S. Listeria monocytogenes-infected bone marrow myeloid cells promote bacterial invasion of the central nervous system. Cell Microbiol. 2005 Feb ;7(2):167-80.

135. Chang YC, Stins MF, McCaffery MJ, Miller GF, Pare DR, Dam T, Paul-Satyaseela M, Kim KS, Kwon-Chung KJ, Paul-Satyasee M. Cryptococcal yeast cells invade the central nervous system via transcellular penetration of the blood-brain barrier. Infect Immun. 2004 Sep ;72(9):4985-95.

136. Greiffenberg L, Goebel W, Kim KS, Weiglein I, Bubert A, Engelbrecht F, Stins M, Kuhn M. Interaction of Listeria monocytogenes with human brain microvascular endothelial cells: InlB-dependent invasion, long-term intracellular growth, and spread from macrophages to endothelial cells. Infect Immun. 1998 Nov ;66(11):5260-7.

137. Grab DJ, Nikolskaia O, Kim YV, Lonsdale-Eccles JD, Ito S, Hara T, Fukuma T, Nyarko E, Kim KJ, Stins MF, Delannoy MJ, Rodgers J, Kim KS. African trypanosome interactions with an in vitro model of the human blood-brain barrier. J Parasitol. 2004 Oct ;90(5):970-9.

138. Marra A, Brigham D. Streptococcus pneumoniae causes experimental meningitis following intranasal and otitis media infections via a nonhematogenous route. Infect Immun. 2001 Dec ;69(12):7318-25.

139. Kim KS. Microbial translocation of the blood-brain barrier. Int J Parasitol. 2006 May 1;36(5):607-14.

140. Rubin LL, Staddon JM. The cell biology of the blood-brain barrier. Annu Rev Neurosci. 1999 ;2211-28.

141. Rüffer C, Strey A, Janning A, Kim KS, Gerke V. Cell-cell junctions of dermal microvascular endothelial cells contain tight and adherens junction proteins in spatial proximity. Biochemistry. 2004 May 11;43(18):5360-9.

142. Stins MF, Badger J, Sik Kim K. Bacterial invasion and transcytosis in transfected human brain microvascular endothelial cells. Microb Pathog. 2001 Jan ;30(1):19-28.

143. Folk JE, Chung SH. Adv. Enzymol. 1993 ;38:109-191.

144. Haigler H, Maxfield F, Willingham M, Pastan I. Dansylcadaverine inhibits internalization of 125I-epidermal growth factor in BALB 3T3 cells. J. Biol. Chem. 1980 Feb 25;255(4):1239-1241.

145. Rikihisa Y, Zhang Y, Park J. Inhibition of infection of macrophages with Ehrlichia risticii by cytochalasins, monodansylcadaverine, and taxol. Infect. Immun. 1994 Nov 1;62(11):5126-5132.

146. Batty S, Chow EMC, Kassam A, Der SD, Mogridge J. Inhibition of mitogen-activated protein kinase signalling by Bacillus anthracis lethal toxin causes destabilization of interleukin-8 mRNA. Cell Microbiol. 2006 Jan ;8(1):130-8.

147. Drysdale M, Olson G, Koehler TM, Lipscomb MF, Lyons CR. Murine innate immune response to virulent toxigenic and nontoxigenic Bacillus anthracis strains. Infect Immun. 2007 Apr ;75(4):1757-64.

148. Dalhammar G, Steiner H. Characterization of inhibitor A, a protease from Bacillus thuringiensis which degrades attacins and cecropins, two classes of antibacterial proteins in insects. Eur J Biochem. 1984 Mar 1;139(2):247-52.

149. Williams PL, Leib SL, Kamberi P, Leppert D, Sobel RA, Bifrare Y, Clemons KV, Stevens DA. Levels of matrix metalloproteinase-9 within cerebralspinal fluid in a rabbit model of coccidioidal meningitis and vasculitis. 2002 ;186:1692-95.

150. Leppert D, Lindberg RL, Kappos L, Leib SL. Matrix metalloproteinases: multifunctional effectors of inflammation in multiple sclerosis and bacterial meningitis. Brain Res Brain Res Rev. 2001 Oct ;36(2-3):249-57.

151. Fasano A, Baudry B, Pumplin WD, Wasserman SS, Tall BD, Ketley JM, Kaper JB. Vibrio cholerae produces a second enterotoxin, which affects intestinal tight junctions. Proceedings of the National Academy of Sciences of the United States of America. 1991 ;88:5242-46.

152. Lu R, Wang W, Uzzau S, Vigorito R, Zielke HR, Fasano A. Affinity purification and partial characterization of the zonulin/zonula occludens toxin (Zot) receptor from human brain. J Neurochem. 2000 Jan ;74(1):320-6.

153. Azghani AO, Gray LD, Johnson AR. A bacterial protease perturbs the paracellular barrier function of transporting epithelial monolayers in culture. Infect Immun. 1993 Jun ;61(6):2681-6.

154. Meyer MA. Neurologic complications of anthrax: a review of the literature. Arch Neurol. 2003 Apr ;60(4):483-8.

155. Dixon TC, Meselson M, Guillemin J, Hanna PC. Anthrax. N Engl J Med. 1999 Sep 9;341(11):815-26.

156. Stearns-Kurosawa DJ, Lupu F, Taylor FB, Kinasewitz G, Kurosawa S. Sepsis and pathophysiology of anthrax in a nonhuman primate model. Am J Pathol. 2006 Aug ;169(2):433-44.

157. Chung M, Jorgensen SC, Popova TG, Bailey CL, Popov SG. Neutrophil elastase and syndecan shedding contribute to antithrombin depletion in murine anthrax. FEMS Immunol Med Microbiol. 2008 Dec ;54(3):309-18.

158. Chitlaru T, Gat O, Grosfeld H, Inbar I, Gozlan Y, Shafferman A. Identification of in vivo-Expressed immunogenic proteins by serological proteome analysis of the Bacillus anthracis secretome. Infect. Immun. 2007 Jun ; 75(6):2841-52.

CURRICULUM VITAE

Dhritiman V. Mukherjee grew up in Durham, North Carolina and received a Bachelor of Art Degree in Experimental Psychology from The University of North Carolina at Chapel in 2000. Soon after graduation he started working for UNC-Chapel Hill Bowles Center for Alcohol Studies in the school of medicine, were he conducted preclinical Psychogenetics Research to identify genes that increase the risk of alcohol-related problems. He continued on to complete 1 year of graduate/medical course work in Neuroscience and worked for 2 years at The Uniformed Services University of the Health Sciences. He then earned a Masters of Science Degree from George Mason University in 2007. Currently, he is a graduate research assistant at George Mason University, Center for Biodefense and Infectious Diseases, working on research prophylactic measures against anthrax meningitis.